
Guidance for the experimental tank testing of wave energy converters



Grégory Payne
The University of Edinburgh
Version: **01b**
22/12/2008

Abstract

Experimental tank testing is a key aspect of wave energy conversion research. The performance of designs can be assessed in an accessible and controlled environment and at a fraction of the cost of sea trials.

There are many different ways to conduct experiments and it is beyond the scope of this document to cover them all. Instead, the author would like to raise readers' awareness on several key aspects of wave tank testing for wave energy conversion. These have been divided into three categories:

- **Model making:** construction techniques, scaling considerations instrumentations.
- **Measurements:** wave measurement, measurement of model motions, data processing (mainly focussed on Fourier analysis).
- **Wave generation:** deterministic and non-deterministic methods, wave tank calibration and phase locking.

This document is based on tank testing practices that have been developed over the years at the University of Edinburgh. As such it is focused on the use of equipment that has been developed by the University of Edinburgh and Edinburgh Designs Ltd.

Contents

Contents	iii
1 General considerations	1
1.1 Introduction	1
1.2 Description of experiments	1
1.3 Duration of experiments	2
1.3.1 Start-up period	2
1.3.2 Record length	3
2 Physical model	5
2.1 Scaling	5
2.1.1 Practical implications of Froude scaling on power take-off modelling	6
2.1.2 Froude scaling overview	7
2.1.3 Scale issues with Oscillating Water Column devices	8
2.2 Model design and construction considerations	8
2.2.1 Buoyancy and ballasting	8
2.2.2 Laminated construction	10
2.2.3 Corrosion	10
2.2.4 Power take-off	11
2.2.5 Sensors	12
2.3 Signal processing	15
3 Measurements	17
3.1 Measurements in the context of Fourier analysis	17
3.1.1 Aliasing	18
3.1.2 Frequency resolution	19
3.1.3 Periodicity of the signal	21
3.1.4 Fast Fourier Transform	22
3.2 Measuring waves	22
3.2.1 Hardware	22
3.2.2 Two-dimensional wave reflection	24
3.2.3 Multidirectional wave spectra	26
3.3 Wave height and period parameters	30
3.3.1 Height parameters	31
3.3.2 Period parameters	32
3.3.3 Time domain versus frequency domain parameters	33
3.4 Video motion tracking device	33
3.4.1 System description	34
3.4.2 User guidance	34
4 Wave generation	37
4.1 The deterministic approach	38
4.1.1 Random phase method	38

4.1.2	Pros and cons of the deterministic approach	38
4.2	The non-deterministic approach	38
4.2.1	Random complex spectrum method	38
4.2.2	White noise filtering method	39
4.2.3	Pros and cons of the non-deterministic approach	39
4.3	Wave tank calibration	39
4.4	Phase locking	40
4.4.1	General considerations	40
4.4.2	Wave generation considerations	42
	References	44

General considerations

1.1 Introduction

Tank testing is a key stage of the development of wave energy converters. It allows the assessment of the performances of a design in an accessible, controlled and repeatable environment at only a small fraction of the cost of sea trials.

There are many quantities that can be measured while carrying out tank testing and consequently many different ways to conduct experiments. It is beyond the scope of this document to cover all of these. Instead, the author would like to raise awareness on several key aspects of wave tank testing.

This document reflects mainly tank testing practices that have been developed over the years at the University of Edinburgh. As such it is focused on wave energy applications and on the use of equipment that has been developed by the University of Edinburgh and Edinburgh Designs Ltd.

1.2 Description of experiments

As obvious as it may sound, it is of prime importance to make a detailed description of experiments. Measurement time series are of little use without an accurate description of what they correspond to and under which conditions they have been obtained. This is even more true if the experimental data are to be used by a third party. An experiment description should be comprehensive enough so that it is possible for another user not involved in the original experiment to repeat it and to obtain the same results. It is virtually impossible to give an exhaustive list of all the parameters and information which should be recorded, simply because the range of these varies from one type of experiment to another. The most important ones are however listed below.

Tank description: geometry (ideally with a scaled plan view), water depth.

Description of the model: geometry, working principle, power take-off mechanism, mooring details.

Position of the model in the tank: in the case of a free-floating device, take note of the position of the mooring anchors.

Wave generation: type and number of paddles (pistons or flaps), generation technique (see section 4 p.37), control frequency.

Name and details of the person who carried out the experiment

Wave Measurement hardware: see section 3.2.1 (p.22).

Wave measurement technique: reflection, directional spectrum see section 3.2 (p.22).

Photos and videos: These are extremely useful because they document the experiments with a very high ‘density’ of information.

Wave tank calibration file: some wave tanks require a calibration file to generate waves (see section 4.3 p.39).

Sensors calibration data: they relate the voltage recorded with the actual value of the physical quantities measured. They also provide information on the linearity of the sensors which can be of importance when analysing measurement. In particular, wave gauge calibration data should be recorded.

Sampling frequencies and synchronising details of the data acquisition system: see section 3.1 (p.17).

Record length: see section 1.3.1.

Start-up period: see section 1.3.2.

Target wave spectrum: this can include the input file to the wave-maker control system.

1.3 Duration of experiments

The duration of an experiment in a wave tank can be divided into three parts, the start-up period, the record length (or sampling period) and the eventual settling time if another experiment is to be run straight after. The latter is the most trivial, as it corresponds to the time required for the water to become still. When using absorbing wave-makers, this typically takes under one minute. The start-up period and the record length depend on the nature of the experiment and on the wave tank.

1.3.1 Start-up period

Most wave-making systems have a ramp-up period during which the command signal goes from 0 to 100% of its target values. This is to avoid putting too much strain on wave-makers and on their drive train. This ramp-up period is likely to scale with the size of the wave-makers - typically it is 4 s in the Edinburgh Curved Tank which has a nominal scale of $1/100^{th}$. The ramp-up time has to be taken into account when deciding on a start-up period but it is not the only consideration as even after the ramp-up, the first few waves tend to be unreliable.

For most experiments, it is desirable to have a start-up period long enough so that the experimental conditions reach steady state. How long is ‘long enough’ depends on the tank and model characteristics. Even for similar experiments, different labs have different start-up periods. This is illustrated by Thompson and Long (1987): within the framework of the International Association for Hydraulic Research, the same experiment was commissioned to different labs. For regular wave experiments, the start-up periods of the various participants ranged from 33 to 100 wave periods. A typical start-up period used in the Edinburgh Curve tank is 30 s.

Specific experiments can require specific start-up periods, it is the case for a free floating model with compliant mooring. The mean drift force of the incoming wave slowly ‘pushes’ the model towards the beaches and depending on the mooring stiffness, it can take some time before the model reaches a stable position. Another example is when measuring waves in a wave flume with the primary consideration that the measurements are not affected by reflected waves. Depending on the wavelength used, the length of the flume and the position of the wave probe(s), the time available to make the measurements before the waves reflected off the beach interfere with it can be short. It is then important to keep the start-up period as short as possible.

1.3.2 Record length

Again, the record length is largely case specific. With regular waves, one wants to record as many integer periods of whatever oscillating phenomenon happening during the experiment. This is to do with Fourier analysis and is explained in more detail in section 3.1 (p.17). The longer the record the finer the frequency resolution of the Fast Fourier Transform. A simple approach with deterministic wave-making systems (see section 4.1 p.38) is to use the repeat period of the wave generation command signal as the record length. In the Edinburgh Curve Tank it is typically 64 s which might lead to too long experiments if many wave periods are to be investigated. On the other hand, some physical phenomena evolve very slowly compared to the wave period and if they are to be captured fully, the record length needs to be long enough. This is the case for example of roll instability of a floating body. It can be induced by the heave-roll coupling through the roll hydrostatic restoring moment. More information on this topic can be found in (Liaw, 1994). It was observed in the Edinburgh Curved Tank when testing the Sloped IPS buoy (Payne et al., 2008). The phenomenon was not obvious from the beginning of the run. It slowly built up and it took about 1 min before it was at its full amplitude.

For irregular waves, the record length depends mainly on whether the wave generation system is deterministic or non-deterministic (see section 4 p.37).

Physical model

A physical model is used in a wave tank to investigate at scale the behaviour of a wave energy converter concept. In most cases some aspects of the full-scale device are simplified in the scaled model. For the power take-off system an electromagnetic damper might for example be used in place of the full-scale hydraulic system. Model tank tests are typically used to investigate the following points:

- Power capture characteristics
- Hydrodynamics
- Power take-off principle and associated control
- Moorings

2.1 Scaling

Generally speaking, in the mechanical interactions between fluids and solids, three kinds of forces are of comparable importance. These are associated with inertia F_i , gravitation F_g and viscosity F_v .

$$F_i \propto \rho U^2 l^2 \quad (2.1)$$

$$F_g \propto \rho g l^3 \quad (2.2)$$

$$F_v \propto \mu U l \quad (2.3)$$

where U is the fluid velocity, g the gravitational acceleration, l the length characterising fluid/solid interaction phenomenon and μ is the dynamic viscosity.

Depending on the phenomenon investigated, the relative magnitude of those forces varies. It is useful to quantify their relative importance. This is typically done using two non-dimensional quantities: the Froude number Fr and the Reynolds number Re .

$$Fr = \frac{U}{\sqrt{gl}} \propto \frac{F_i}{F_g} \propto \frac{\text{inertial force}}{\text{gravitational force}} \quad (2.4)$$

$$Re = \frac{Ul}{\nu} \propto \frac{F_i}{F_v} \propto \frac{\text{inertial force}}{\text{viscous force}} \quad (2.5)$$

where ν the kinematic viscosity ($\nu = \mu/\rho$).

Ideally, when designing scaled model testing, it is desirable to retain the same balance between inertial, gravitational and viscous effects as that of the full-scale phenomenon. This implies ensuring that the values of both Fr and Re at model scale are the same as the full-scale ones. In practice, this is usually difficult to achieve, especially at small scale. As an example, if we consider the investigation of the forward motion of a ship using a $1/100^{th}$ scale model in a towing tank. Assuming that the gravitational acceleration g is the same in both model and full-scale conditions, if Fr is to be kept constant, according to (2.4), the value of the forward speed U , at model scale has to be $1/10^{th}$ of the full-scale one. Now assuming that the fluid used with the model is the same as in full-scale, ν is the same in both model and full-scale conditions. If Re is to be kept constant, according to (2.5), the value of U at model scale has to be 100 times that of the full-scale value. The obvious way to overcome these conflicting requirements would be to increase g and/or decrease ν . This would involve running the model experiments in a centrifuge and/or using fluids whose viscosities are lower than that of the full-scale one. Unfortunately this kind of experimental set up is not practical for tank testing of wave energy devices, where tanks are too large to fit in centrifuges and are filled with water.

During the interaction between waves and solid bodies, the effects of viscosity are generally felt in the boundary layer, in the close vicinity of the water-body interface. In the rest of the fluid volume, viscous effects are generally negligible. The relative influence of viscous forces will thus be greater for complex WEC geometries that have large wetted-surface areas in relation to their immersed volumes compared with more compact WEC shapes that have lower ratios of wetted-area to volume. For many tank-scale WECs, the net influence of viscous forces on body motions is small and Froude scaling can be assumed to be satisfied. This assumption that the ratio of inertial forces to gravitational forces is the same at model- and at full-scale generally leads to conservative predictions of full-scale device behaviour. A good introduction to the very important topic of scale can be found in chapters 1 and 2 of Newman (1977).

2.1.1 Practical implications of Froude scaling on power take-off modelling

For wave energy applications, one of the key consequences of Froude scaling is the scaling law of wave power.

Let s be the geometric scale between model and full-scale conditions. From (2.4) if Fr and g are constant, then U scales with \sqrt{s} . In terms of dimensions:

$$[U] = \frac{[L]}{[T]} \quad (2.6)$$

where $[U]$, $[L]$ and $[T]$ are the dimensions of velocity, length and time respectively. So time scales also with \sqrt{s} .

The dimensions of power are:

$$[P] = \frac{[M][L]^2}{[T]^3} \quad (2.7)$$

where $[M]$ is the dimension of mass. As mass is proportional to volume, $[M]$ scales with s^3 , and thus, power scales with $s^{3.5}$.

Depending on the size of the models and tanks used, the model scales are typically of the order of $1/30^{\text{th}}$ to $1/100^{\text{th}}$. Assuming a full-scale power take-off rated at 1 MW, the model power rating would be of the order of 0.1 to 7 W. This means that in order to simulate full-scale behaviour accurately, power dissipation due to friction losses in the model power take-off, should be kept very low, ideally, down to the ‘milliwatt’ level. It is therefore important to design models with very low friction bearing between moving parts. Hydrostatic bearings have very low friction but tend to be more complex to implement than bush or ball bearings. Taylor and Mackay (2001) have successfully used water fed hydrostatic bearings on a model power take-off. Further information on hydrostatic bearings can be found in Stansfield (1970).

2.1.2 Froude scaling overview

Using the same reasoning as in section 2.1.1 the scaling of various quantities of interest can be derived. Some of these are shown in table 2.1.

Quantity	Scaling
wave height and length	s
wave period	$s^{0.5}$
wave frequency	$s^{-0.5}$
power density	$s^{2.5}$
linear displacement	s
angular displacement	1
linear velocity	$s^{0.5}$
angular velocity	$s^{-0.5}$
linear acceleration	1
angular acceleration	s^{-1}
mass	s^3
force	s^3
torque	s^4
power	$s^{3.5}$
linear stiffness	s^2
angular stiffness	s^4
linear damping	$s^{2.5}$
angular damping	$s^{4.5}$

Table 2.1: Froude scaling law for various quantities. s is the geometric scale. When the scaling is 1, it means that the value of the quantity is not affected by scale. The term ‘Power density’ refers to power per unit length.

2.1.3 Scale issues with Oscillating Water Column devices

In Oscillating Water Column (OWC) wave energy converters, the displacement of the water column is driven by hydrodynamic effects. The power take-off mechanism relies on aerodynamics as the air in the OWC chamber is forced back and forth through a turbine. This combination of hydrodynamics and aerodynamics renders scaling considerations for OWCs more complex than standard Froudean scaling.

The hydrodynamics interactions between waves and the OWC are dominated by inertial and gravitational forces. The aerodynamics of the air volume of the OWC chamber is dominated by the compression force F_c . Assuming volume deformation of the chamber in one dimension and reversible and adiabatic conditions:

$$F_c \propto P_0 \kappa l^2 \quad (2.8)$$

where P_0 is the initial air pressure, κ the isentropic exponent and l the characteristic length (Weber, 2007). Both inertia and pressure forces act as restoring forces in the heaving motion of the water column. Maintaining the same balance between these two at model and full-scale involves keeping the ratio:

$$\frac{F_i}{F_c} \propto \frac{\rho U^2}{P_0 \kappa} \quad (2.9)$$

constant. From (2.9) and (2.4), keeping both the F_i/F_c ratio and the Froude number constant involves keeping the ratio:

$$\frac{\rho g l}{P_0 \kappa} \quad (2.10)$$

constant which is difficult in practice. One approach to address this issue is to design a model with different scales above and below the waterline. In other words, the horizontal cross section of the chamber remains the same but the top part of the chamber can be made higher to increase its volume. This has been tried by Maunsell and Murphy (2005). More information on the topic of OWC scaling can be found in Weber (2007) on which this treatment is based.

2.2 Model design and construction considerations

The recommendations in this section mainly reflect the model making approach developed by the University of Edinburgh. There are many other techniques to build models and the ones presented here are not claimed to be the only good ones but have been found to work well for the various models made over the years at the University of Edinburgh.

2.2.1 Buoyancy and ballasting

Closed cell plastic foam is an attractive material to make buoyancy units. The brand that the University of Edinburgh has been using is Divinycell. The main advantage of this material is its closed cell nature which allows it to be used in the water without any coating. The water penetration is limited to the cells of the material surface as they have been cut open by cutting

or machining. Therefore water does not penetrate deeper than a millimetre. Divinycell comes in various densities: 45, 60, 80, 100, 130, 160, 200 and 250 kg/m³. It is easy to machine with sharp tools and appropriate cutting speed. It is much tougher than polystyrene and can be used without coating for most application. When resistance to sharp impact is an important consideration, Divinycell can be coated with a low viscosity epoxy resin.

The static and dynamic behaviours of a floating body are not only affected by its shape but also by its mass distribution. It is therefore desirable to be able to easily alter the mass distribution of a model. One way to do so is to incorporate a set of hollow tubes in the model. Those tubes, typically spread parallel through the model are open at both ends so that ballast rods can be fitted into them. The tubes are typically made of PVC and the ballast rods of stainless steel. A groove made at each end of the rod is fitted with an o-ring whose outer diameter, once in place, is just over the inner diameter of the tubes. The rods can be made of different length (and thus different mass) and can easily be slid in and out of the tubes with the o-rings friction retaining them in place. Figure 2.1 shows the different details of this technique.



Figure 2.1: *Ballast weight arrangement in a Divinycell buoyancy unit. The holes are lined with grey PVC tubes. The left most bar is shown not fully inserted in the tube with the o-ring not fitted to show the groove. On the middle bar the o-ring is fitted and the right most bar is fully inserted in the tube.*

2.2.2 Laminated construction

Some of the materials used for model construction come only in slabs of limited thickness. Furthermore, it is often easier to cut or machine profiles on materials which are not too thick. On the other hand, the dimensions of some wave energy converter model parts tend to be bulky compared with the thickness of the raw materials they are to be made of. This is typically the case when one wants to make buoyancy units out of Divinycell. A convenient method to overcome this issue is to use laminated construction by stacking matching profiles to reach the desired width. The profiles can either be glued together or held together by structural braces, typically aluminium bars, that run perpendicularly across the profiles. The latter option is more flexible as it allows the width of the construction to be easily altered. The design is however more complicated as it requires holes for the braces to be accurately machined in each profile section. It is sometime convenient to cut each profile section roughly to the right shape, to then stack the profiles and to finally sand the whole part down to the desired shape so that the assembly is seamless. Figure 2.2 shows the gluing stage.



Figure 2.2: *Laminated construction of a buoyancy unit. The Divinycell profiles to be glued are on the right hand side of the picture. The two vertical alloy bars with white endings are structural braces used to attached the float to the other parts of the model. They also ensure that the profiles are well aligned with each others. The hole pattern is for ballasting (see figure 2.1).*

2.2.3 Corrosion

Most wave energy converters model will inevitably have metal parts. Although water in wave tanks is usually not sea water, corrosion has to be taken into consideration. The most obvious solution is to use stainless steel, but this material is expensive and more difficult to machine than aluminium alloys. Models often end up being made of several metals that usually include

stainless steel and aluminium. The former being used mainly for fastener and the latter for structure.

Aluminium is actually more ‘active’ than iron and as such it will oxidise more readily. As it does so, a layer of aluminium oxide forms which strongly inhibits further oxidation. Aluminium corrosion should therefore not be too big an issue, especially if the model is taken out of the water regularly. If it is exposed to water for a prolonged period of time it eventually rusts, producing a white powdery coat. Aluminium can be protected by anodising. This electro-chemical process coats the metal with a thin layer of aluminium oxide which is both very hard and corrosion resistant.

For some applications, steel has to be used underwater. This is usually for its electromagnetic characteristics which are very different from that of stainless steel or aluminum. In this case, corrosion can be avoided by introducing inhibitors in the tank water or by coating. The most common type of protective coating is achieved by galvanisation. After this process, the metal is covered by a layer of zinc carbonate that offer a good resistance to corrosion. The drawback of galvanising is that the resulting surface finish is rather rough and the coating does not always follow very well fine details of the part geometry, especially threads. To avoid this issue, chrome or nickel plating can be used instead.

When using a combination of two different metals in contact with each other and with water, corrosion can be greatly accelerated by galvanic effect. For galvanic corrosion to happen, the two metals must be in direct contact and exposed to the same body of water. This forms a galvanic cell. The most noble (or passive) metal behaves as a cathode whereas the most active behaves as an anode where oxidation takes place. The ions travel in the water and the electrons travel through the direct contact between the two metals. The larger the difference in electrode potentials between the two metals, the more severe the rate of oxidation is.

2.2.4 Power take-off

Scale modelling of power take-off mechanisms is not straight forward. The technologies suitable for full-scale devices usually do not lend themselves to down-scaling. This is mainly due to the scaling factor of power in Froude scaling (see section 2.1.1, p.6). This is the case for hydraulic rams which are an attractive first stage for full-scale power-offs but whose friction losses make them unsuitable for scaled models.

The ideal model power take-off dynamometer provides a means of applying arbitrarily defined forces between the wave-driven and the reactive body-elements of the WEC. It is convenient if the forces can be accurately varied as linear functions of a control voltage or current. The system should have as few additional mechanical artifacts as possible. For example, friction losses and mechanical backlash should be minimised. Typically, to represent pure damping, the force provided by the dynamometer will be configured to be proportional to the relative velocity of the wave-driven motions of the WEC body elements and will act in opposition to them. In order

to explore maximum power-capture techniques, there should be few limitations on the kind of control algorithm that can be implemented. Where it is possible to use them, amplifier-driven DC electric-motors provide the best means for implementing this kind of control. The best kind of DC motor is the brushless type as made by Aeroflex - although their limited angular range may be unsuitable for many models. DC motor force is directly proportional to current, so current-amplifiers should be used. For accurate results (unless a brushless motor is used) some means of measuring the motor force may be required. Typically this will involve the incorporation of strain-gauged components in the force path. The flexibility offered by these kinds of dynamometer systems often makes it possible to drive the WEC in calm water in order to measure and calculate its hydrodynamic coefficients - the added mass and the radiation damping.

Some mechanical dampers can be calibrated with reasonable accuracy. They can then be implemented in model power take-offs to carry out quantitative measurements. It should be noted however that when using this method, the resisting force applied to the prime mover cannot be controlled with the same freedom as with DC motors. Moreover, that force is often not fully linear with the prime mover displacement or velocity. In the case of OWC, an equivalent approach relies on aerodynamic dampers. These are typically carpet sheets or slit shims whose flow to pressure characteristics can be calibrated (Lucas et al., 2007). Experimenters should be aware that carpet characteristics are affected by the moisture level of the carpet.

Cruder power take-offs can also be used. This depends on the stage of investigation considered. For early experimental tests, one might only be interested in qualitative assessments of the impact of the power take-off resistance to the prime mover on the model behaviour. In this case, some kind of simple friction-brake may be suitable.

It is important to emphasise that the quality of the model power take-off affects directly the range and the quality of the measurements that can be carried out. The technology chosen should therefore be appropriate to the scope of the model testing investigation.

2.2.5 Sensors

2.2.5.1 Sensor technology

Displacement and velocity sensors should ideally be contact-free so that they do not interfere with the motions they are measuring. Alternatively they should be low friction.

A reasonably cheap and common option is to use potentiometers. These can be utilised for both rotational and linear motions. The potentiometers should be carefully chosen to be low friction (some are even non-contact) and to have an 'electrical angle' suitable to the motion range to be measured. For translational motions, 'string potentiometers' can be used. These can be seen as electronic tape measures. They measure linear displacement by means of a string which is wound onto a drum by a rotational spring. The measuring drum is coupled to a multi-turn potentiometer. When using these, one should ensure that the spring force of the sensor is either negligible compared with the other forces involved or taken into account.

An alternative to potentiometers are encoders. These output a digital signal but tend to be more expensive.

When dealing with rotational motions of small amplitudes ($\pm 20^\circ$) the resolution provided by potentiometers or encoders can prove to be limited. In this case, Rotary Variable Differential Transformers (RVDT) can be used. They consist of a primary coil and a set of two secondary coils. The three coils are stationary. The primary coil is energised by an AC source. The secondary coils are electromagnetically coupled to the primary through a rotating iron core connected to the input shaft. The electromagnetic coupling is proportional to the angle of the input shaft. The voltage induced in the secondary coils is proportional to the rotation angle. These two coils are connected so that they are 180° out of phase. The voltage from the secondary coils is therefore the difference between the voltage of each of the two. This differential approach makes the resulting voltage less sensitive to variations of the voltage in the primary coil. The range of RVDTs is typically $\pm 30^\circ$ and they are non-contact. It should be noted however that they are more expensive than potentiometers and that they require more 'conditioning' electronics since the input and output voltages are AC. The variable differential transformer principle can also be applied to measure linear motion. In this case the sensors are called LVDTs where the L stands for Linear. As for RVDTs, LVDTs tend to have short measurement range. A cheaper alternative to RVDTs and LVDTs are the 'Blade' non-contact sensors manufactured by the company Gill Sensors (www.gillsensors.co.uk). These are inductive and can measure both linear and angular motions.

To measure forces there are two main technologies: strain gauges and Piezoelectric sensors. The latter are made of Piezoelectric materials (crystal or ceramic) which source electric charge when squeezed and sink it when relaxed. As an analogy we can compare a Piezoelectric crystal with a wet sponge, with water representing electric charge. The voltage created is directly proportional to the force or strain applied to the sensor. Piezoelectric materials are very stiff and therefore hardly deform when under compression. On the other hand, these sensors are not well suited for static measurements. Under static pressure, the voltage they generate tends to drift with time.

Strain gauges can be used to measure force indirectly by measuring the strain of a material (typically a metal) induced by the force applied to it. Strain gauges are typically made of a metallic foil pattern laid onto a flexible insulating substrate. The whole assembly is glued onto the material so that the strain experienced by the material is transferred to the gauge. The resistance of the gauge varies with strain. It decreases with compression and increases with tension. Resistance also varies with temperature. Almost invariably sets of four strain gauges are used in the Wheatstone Bridge configuration to null the effects of temperature. Strain gauges can also be made of semiconductors, exploiting the piezoresistive effect. These gauges are more sensitive than foil gauges but they also tend to be more expensive, more sensitive to temperature and more fragile.

When designing a strain gauge sensor it is important to know the range of forces that is to be measured. From these data, the range of the strain gauge as well as the nature and shape of the material to be deformed can be worked out. Once the sensor is assembled, it needs to be calibrated.

Piezoelectric sensors are very stiff but generally need to be in compression. This is not always easy to arrange. Strain gauge sensors on the other hand can measure compressive and tensile forces but they deform more under the force they measure. They are typically designed for a maximum deflection of one micro-strain (strain $\times 10^6$) under maximum load. If they are to be used as part of a servo control loop, one has to be vigilant to avoid low-frequency resonances from the stiffness of the strain gauge sensor coupled to any associated masses or inertias.

2.2.5.2 Sensor implementation

Motion, velocity and force sensors should generally be fitted as closely as possible to the physical phenomenon they are intended to measure. The idea is to avoid corrupting the measurements with mechanical artifacts (such as backlash or excessive friction) from linkages or bearings. Force measurement usually involves the inclusion into the force path of compliant elements whose dimensional changes are captured by strain-gauges or piezo crystals. The effect of the compliance is usually to lower the natural frequency of the system that the sensor forms a part of. Where the force signal is part of a force feedback loop, as might be the case with a power take-off dynamometer, care must be taken to keep the force path mechanically stiff so that resonances are well above the tank wave frequency band. Otherwise it may be difficult to make the system stable.

Sensors that need to be submersed obviously require some form of protection against water ingress. The easiest approach is to source sensors manufactured to be waterproof. Typically, an International Protection rating 68 (IP68) is suitable for continuous immersion in wave tanks. However, when designing bespoke sensors, waterproofing must be done 'in-house'. In the case of strain gauges, the waterproofing must not alter the measurements, so one has to make sure that the stiffness of the waterproofing material is negligible compared with the stiffness of the bar that is to be deformed. Non-acetic silicon rubber potting compound can be used. The non-acetic characteristic is important as most standard silicon compounds release acidic fumes while curing which can lead to severe corrosion problems. To get a neat finish a mould can be used to form the potting. It is also important to spray the mould with a mould-release agent and to clean and degrease thoroughly the surface on which the compound is bind on. The cured potting remains soft and so is susceptible to damage; to address this problem the assembly can be protected by a heat shrink sleeve. The various stages of strain gauge waterproofing are illustrated in figure 2.3.

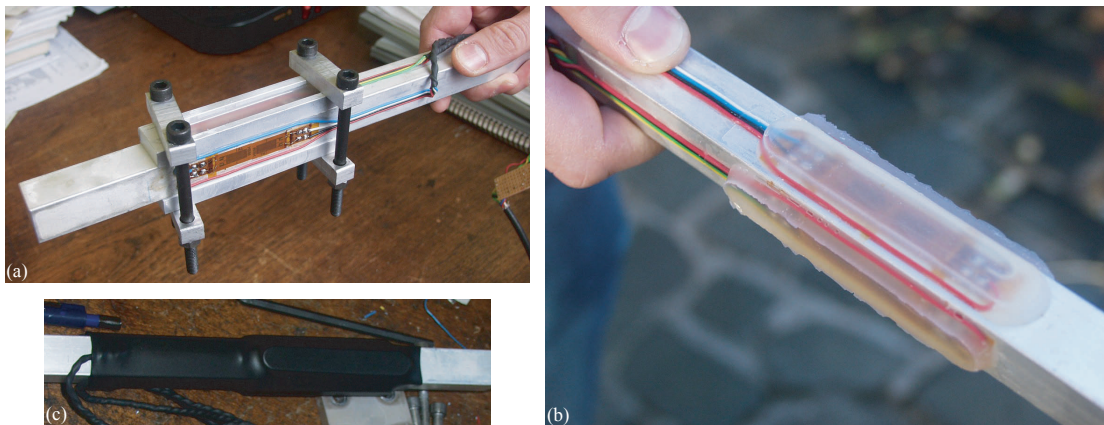


Figure 2.3: *Different stages of strain gauge waterproofing. (a): silicon rubber potting compound is applied using moulds on top and bottom faces of the bar. On the side faces, the bare strain gauges can be seen before waterproofing. (b): all faces have been waterproofed and moulds have been removed. (c): with heat shrink sleeve protection. (All pictures by Jorge Lucas)*

2.3 Signal processing

When putting together a data acquisition system to log measurements from sensors, the aim is always to get as much ‘signal’ and as little ‘noise’ as possible.

Most electrical noise is at frequencies that are very much higher than tank wave frequencies and is reasonably easy to eliminate by the careful use of low-pass filters. However, in the design of electronic instrumentation you also have to be very careful not to pick up some dangerously close to 50 or 60 Hz noise from nearby mains-operated electrical equipment. You must make sure that the design of your instruments eliminates this. An important rule is to never start serious data acquisition until you have checked the signal quality and the comparative amount of ‘signal to noise’. There is only one way to do this, and that is to look at each signal on an oscilloscope whilst the wave and model systems are running at the lowest wave amplitudes that will be used during experiments. You should also check the dynamic range of all of the signals relative to the full-scale range of the data acquisition system. Ideally, to get the best resolution, all incoming signals at maximum value will reach at least two-thirds of the data acquisition maximum. You should also keep checking the signal quality during experiments in case any sensor fails or starts to get wet.

Convention dictates that signals that are to be sampled by a data acquisition system should first be passed through a low-pass filter. Without such filtering, signal components at frequencies greater than half of the data sampling frequency break through into the sampled signal band as ‘aliasing’ (see section 3.1.1, p.18). However, it is likely that you will not always be using the same data sampling frequency so it may be difficult to decide on the best filter cut-off frequency. For long experiments, it might suffice to sample at twice the frequency of the shortest wave component. In another experiment you might want to look at the transient effects of a breaking wave and to therefore sample at a much higher rate - perhaps up to several hundred hertz.

If the signals are very clean, you might not need to use any low-pass filtering. A more conservative approach is to ‘roll-off’ all signals at a frequency around 1 kHz with first-order low-pass filters. These will have little effect on the phases of the much lower frequency wave signals. In any event, after sampling any such phase errors could be subsequently corrected in the frequency domain.

Measurements

The quantities which are of interest to measure in the context of tank testing for wave energy applications are numerous. This section provides guidelines on the generic aspects of tank measurement and focuses on the most commonly measured quantities.

3.1 Measurements in the context of Fourier analysis

Frequency analysis is a widely used technique for investigating phenomena involving water waves. The general idea of Fourier analysis is based on the fact that a periodic function f of period T can be expressed as the sum of its harmonic components:

$$f(t) = a_0 + \sum_{k=1}^{\infty} \left(a_k \cos \frac{2\pi kt}{T} + b_k \sin \frac{2\pi kt}{T} \right) \quad (3.1)$$

where the a_k and b_k are the Fourier coefficients defined by:

$$\begin{aligned} a_0 &= \frac{1}{T} \int_{-T/2}^{T/2} f(t) dt \\ a_k &= \frac{2}{T} \int_{-T/2}^{T/2} f(t) \cos \frac{2\pi kt}{T} dt \quad \text{for } k \geq 1 \\ b_k &= \frac{2}{T} \int_{-T/2}^{T/2} f(t) \sin \frac{2\pi kt}{T} dt \quad \text{for } k \geq 1 \end{aligned} \quad (3.2)$$

By looking at the amplitude of the coefficients one can assess the spectral content of the signal. It is beyond the scope of this document to give an extensive description of Fourier analysis theory. More information on this topic can be found in Newland (2005).

The method commonly used to carry out a spectral analysis of a discrete time series x_p of N samples ($p = 0, 1, 2, \dots, N - 1$) is the Discrete Fourier Transform (DFT) which is defined, using complex notation, as follows:

$$X_k = \frac{1}{N} \sum_{p=0}^{N-1} x_p e^{-i \frac{2\pi kp}{N}} \quad \text{for } k = 0, 1, \dots, N - 1 \quad (3.3)$$

The Inverse Discrete Fourier Transform is given by:

$$x_p = \sum_{k=0}^{N-1} X_k e^{i\frac{2\pi kp}{N}} \quad \text{for } p = 0, 1, \dots, N - 1 \quad (3.4)$$

The DFT is a practical method to estimate the spectrum of a continuous time series. However, it should be borne in mind that the DFT does not output the true continuous spectrum but an estimate of it. The quality of the estimate is directly influenced by the way the continuous time series is sampled.

3.1.1 Aliasing

The sampling frequency used to sample a continuous time series dictates the frequency range and impacts on the quality of the spectrum calculated by the DFT. One should ensure that the sampling frequency is at least twice that of the highest frequency component of the time series.

When sampling at frequency f_s the DFT process is unable to distinguish between components whose frequencies f_1 and f_2 are symmetrical with respect to $f_s/2$: $f_1 \leq f_s/2$ and $f_2 = f_s - f_1$. Figure 3.1 illustrates this phenomenon. It shows two sine waves, one of frequency 0.5Hz and the other of 3.5Hz. The circles represent the sampled data with a sampling frequency of 4Hz. The 3.5Hz sine wave has deliberately been shifted by 180°. It can be seen that the sampled

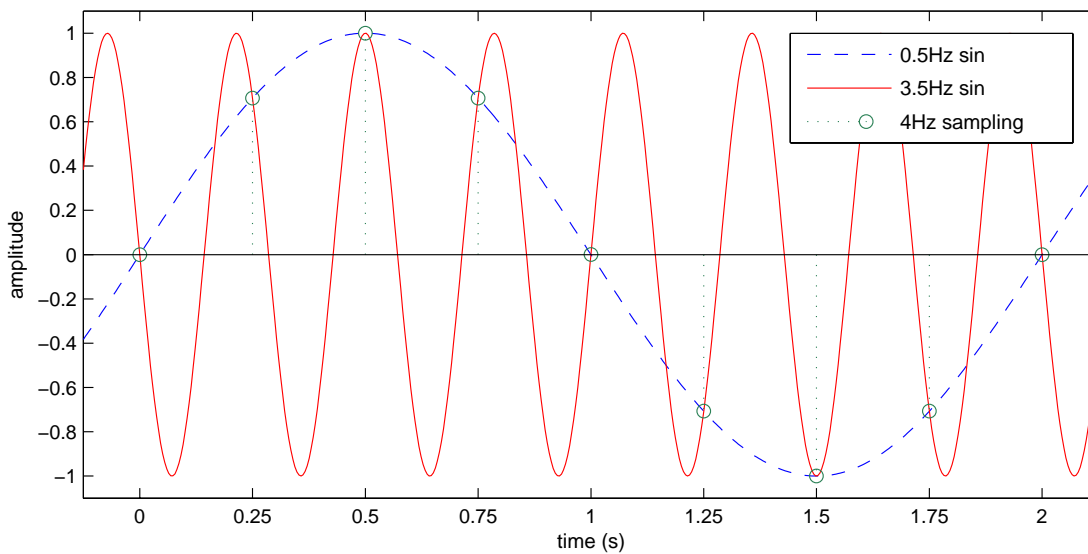


Figure 3.1: Example of aliasing

values are the same for the 0.5Hz and the 3.5Hz sin waves.

In the DFT output, the sum of the measured amplitudes of the two components ends up being equally split between the two frequency components (f_1 and f_2) even if their true respective

amplitudes are different. The outcome is a spectrum symmetrical with respect to $f_s/2$. If the true amplitude of component f_2 is zero, the DFT will output a spectrum with components at frequencies f_1 and f_2 whose amplitudes are equal to half the true amplitude of component f_1 . By doubling the amplitude of DFT component f_1 and discarding DFT components of frequency above $f_s/2$, the true spectrum can be derived. This is however not possible when the amplitude of the true component f_2 is not zero. In this case, the spectrum obtained is distorted and does not suitably approximate the true spectrum. This can be generalised for any numbers of frequency components. The phenomenon is called ‘aliasing’ and $f_s/2$ is referred to as the ‘Nyquist frequency’ or sometimes the ‘folding frequency’. More detail on that topic can be found p.118 of Newland (2005).

To summarise, the sampling frequency has to be chosen so that the Nyquist frequency is above the frequencies of *all* the components of the time series and not only of the ones of interest. A practical way to achieve this is to use an appropriate low-pass filter before sampling the signal.

3.1.2 Frequency resolution

The frequency resolution of the DFT is determined by the sampling duration. To be more specific, in the DFT process, the time series is correlated with sinusoids whose frequencies are integer multiples of the inverse of the sampling duration. In other words, if the time series is sampled for a duration ΔT_{dur} it will be correlated with sinusoids of frequency:

$$f_k = \frac{k}{\Delta T_{dur}} \quad \text{with } k = 0, 1, \dots, N - 1 \quad (3.5)$$

where N is the total number of samples. The frequency resolution of the DFT is therefore $1/\Delta T_{dur}$.

Let us consider a time series that consists of a single sinusoid of frequency f_1 . If the sampling duration is chosen so that f_1 does not correspond to any of the frequencies of the correlation sinusoids (that is if $f_1 \neq f_k$ with $k = 0, 1, \dots, N - 1$), then the amplitude of the true component will be spread over the nearest DFT components. This phenomenon is commonly referred to as ‘spilling’. This is illustrated in figure 3.2 where the time series is a sinusoid of amplitude 1 and frequency $\frac{31}{32}$ Hz. The sample frequency is 32 Hz and the sampling duration is 16 s. It should be noted that for clarity consideration, the spectrum is truncated and does not display the whole frequency range of the DFT.

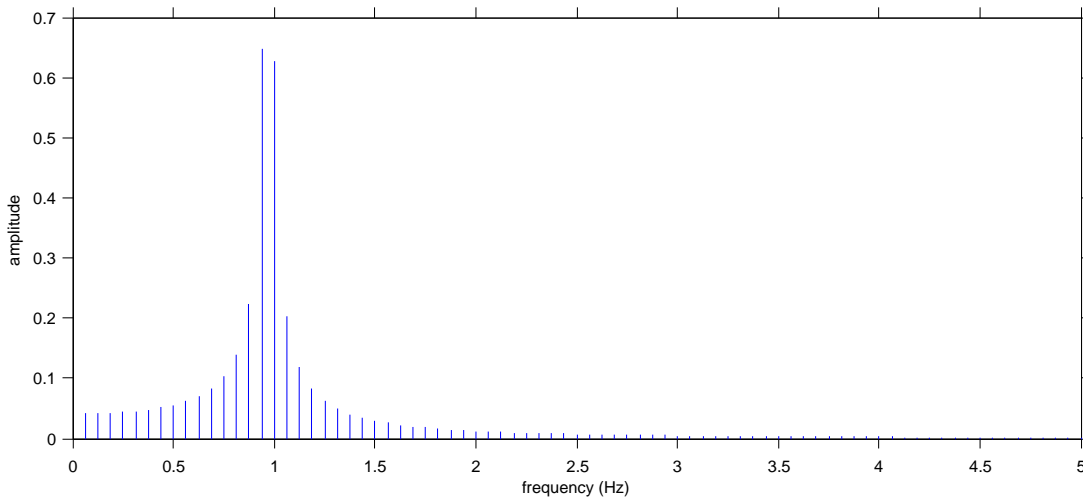


Figure 3.2: *Spectrum exhibiting spilling due to inappropriate sampling duration ($\frac{31}{32}$ Hz signal sampled for 16s at 32Hz)*

When the sampling duration is such that one of the f_k matches f_1 , the resulting spectrum is much ‘cleaner’. This is shown on figure 3.3 where the parameters are the same as for figure 3.2 except for the sampling duration which is here 32s.

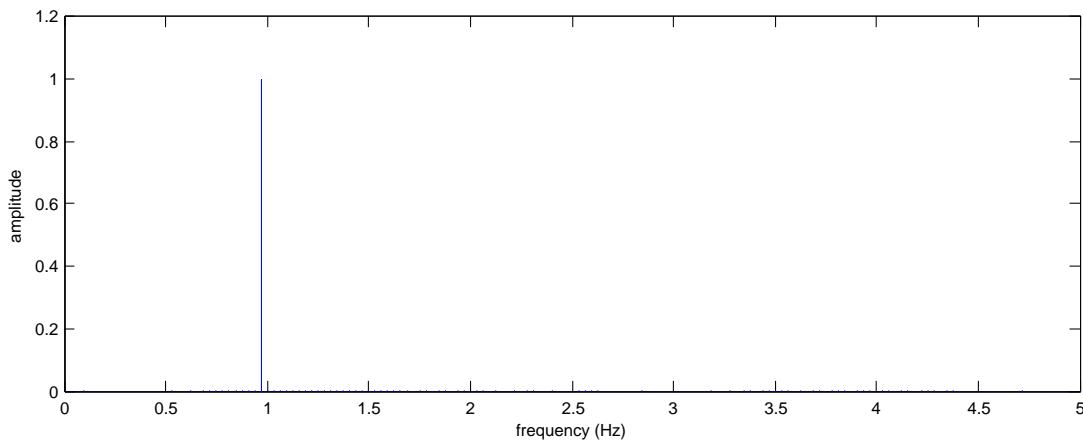


Figure 3.3: *Spectrum without spilling ($\frac{31}{32}$ Hz signal sampled for 32s at 32Hz)*

In order to obtain good quality spectra from DFT, it is recommended to choose a sampling frequency and a sampling duration so that the frequency of each component of the time series analysed is matched by one of the f_k . When the time series is derived from a true natural process, like wave elevation at one point in the ocean, this is not possible because there will be an infinite number of frequency components. In a wave tank however, the command signal sent to the wave makers is usually computed by Inverse Discrete Fourier Transform (IDFT) and

therefore contains only a finite number of frequency components which can be matched by the f_k .

3.1.3 Periodicity of the signal

Theoretically speaking, the DFT performs better if the time series analysed is periodic and if the sampling duration corresponds to an integer multiple of the period. If the wave generation system of the tank is controlled in a deterministic manner (see section 4.1), the sampling duration should be chosen so that it corresponds to an integer multiple of the pseudo period or repeat time of the system. If the signal sampled is not periodic, it is recommended to use a tapered data window to smooth the data at both ends of the sampled time series before carrying out the DFT. A data tapered window is basically a weighing function which gives more importance to the middle of the time series compared to the extremities. It can be seen as ‘making’ the time series ‘look’ more periodic by smoothly bringing the values of both ends to zero. This process is illustrated in figure 3.4 where a cosine tapered window is applied to the time series of a random signal. It should be noted that periodicity ‘enforcing’ by data windowing is done at the cost of distorting data. More information on this topic can be found in chapter 11 of Newland (2005).

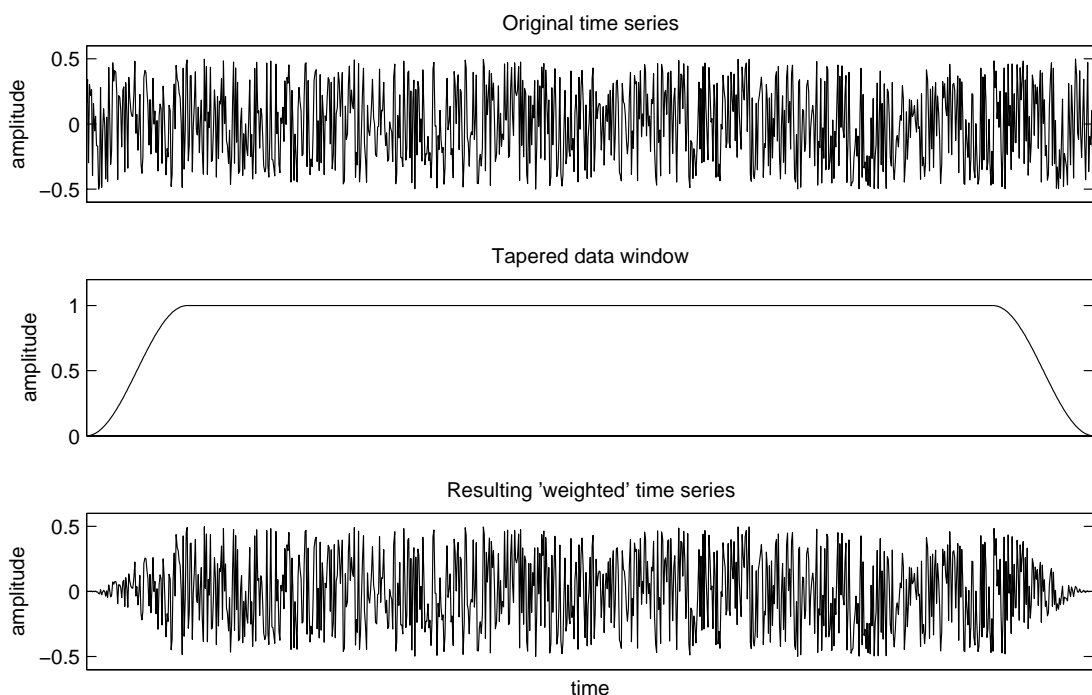


Figure 3.4: Application of a tapered window to a random signal

3.1.4 Fast Fourier Transform

The name Fast Fourier Transform (FFT) refers to an algorithm used to compute the DFT. It was originally introduced by Cooley and Tukey (1965). It is particularly computationally efficient and accurate. It has now become the standard method for deriving the DFT. There are several variations of the FFT algorithm but the most common ones require the number of samples N to be a power of 2. If it is not the case, most algorithms extend the number of samples to reach the nearest power of 2 by ‘adding’ zeros at the end of the original time series. This results in a spilling phenomenon.

3.2 Measuring waves

3.2.1 Hardware

There are several types of wave gauges used to measure waves in wave basins. Here is a brief overview of the technologies available.

3.2.1.1 Float gauge

This technique relies on measuring the vertical displacement of a float following the water surface. Sub-millimetre accuracy has been achieved with this method (see chapter 4 of Nebel (1994)). To avoid following errors, the heave motion of the float should be as close as possible to the vertical motion of water particles. This is achieved by ensuring that the ratio of the float water plan area over the float inertia is as high as possible. The idea is to make sure that the natural frequency of the float in heave is much higher than the frequency of the measured waves. A description of a gauge of this type developed at the University of Edinburgh can be found on p.24.4 of Jeffrey et al. (1976)

3.2.1.2 Capacitance gauge

Wave gauges of this type typically consist of two vertical metal rods partly immersed. One or both of the rods is covered with a thin layer of electrical insulator. The capacitance measured between the two rods is linearly dependant on the immersion depth. Alternatively, the non insulated electrode can be taken away and replaced by the tank electrical ground. More information on capacitance wave gauge working principle can be found in Clayson (1989).

The advantage of this technology is that calibration is fairly stable with time. On the other hand, the insulation layer on the rods can be a source of reliability issues. In order to achieve reasonably high capacitance values, the insulation coating has to be very thin and it can therefore be easily damaged.

3.2.1.3 Water surface following gauge

This technology relies on a servo-drive mechanical system tracking the water surface. It provides an absolute measurement of the water level and is calibration-free.

A prototype of this type of gauge has been built at the University of Edinburgh using a capacitive sensor to detect the water surface. 0.5mm accuracy has been achieved. More information can be found in Spinneken (2004).

3.2.1.4 Ultrasound gauge

Ultrasound waves are beamed vertically downward. They are reflected up by the water surface. The wave height is derived from measuring the time of the 'flight'. This time is inversely proportional to the speed of sound in the air which is affected by environmental quantities such as temperature and humidity. As these are not constant, calibration needs to be carried out regularly.

Two models of ultrasound gauges have been tested at the University of Edinburgh. Static calibration yielded good linearity of the sensors. The error on the linear fitting was found not to exceed 0.03mm. There were however issues with the dynamic performance of the sensors. In regular waves, the signal would break down when waves were too steep. No clear steepness limit could however be established and the wave steepness at which the sensors stopped working properly depended on the wave frequency. As an example, for 1.2Hz waves, the signal broke down when the steepness exceeded 0.36. The maximum sampling frequencies of the sensors were respectively 15Hz and 20Hz which is rather on the low side.

3.2.1.5 Conductive wave gauges

Conductive wave gauges typically consist of two thin, parallel vertical metal rods partly immersed. The water height is derived from the conductivity between the rods which increases with the immersion of the rods. More information can be found in Clayson (1989).

Regular calibration is required as the water conductivity changes. In (Thompson and Long, 1987) it is stated that at the US Army Engineer Waterways Experiment Station, wave gauges are calibrated statically at least twice a day. It states that, ideally the calibration should be dynamic but that given the complexity of this procedure; most laboratories rely on static calibration. It is also recommended to run waves in the tank for a few minutes before calibrating the gauges in order to mix the water to make the water conductivity the same everywhere in the tank.

3.2.1.6 Optical gauge

This technique relies on the principle of triangulation. A spot created by the scattering of laser light at the water surface is detected by an off-axis camera. The images from the camera are

processed to derive the centroid of the spot. The centroid position is transformed into a height value using a polynomial best-fit function established by calibration. This is summarised in figure 3.5 where height measurements are shown for a wave crest (in red) and a trough (in blue).

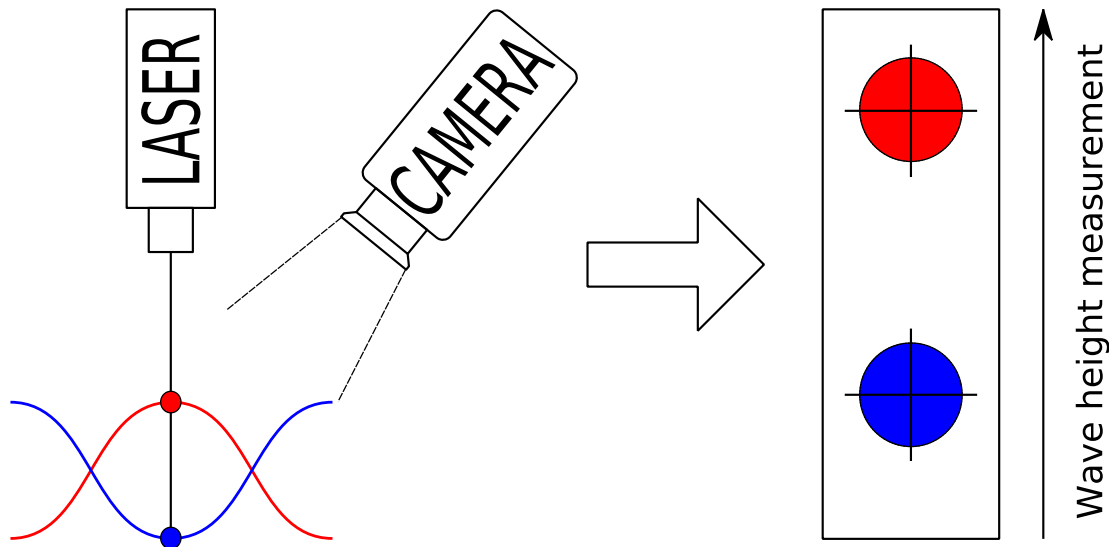


Figure 3.5: Schematic of an optical wave gauge

Optical gauges are non-contact so the measurements are not biased by surface tension as in capacitive and conductive wave gauges which suffer from meniscus effect. Optical sensing allows adjustable resolution, by choice of the camera optics magnification. Sub-millimetre accuracies have been achieved on waves with more than 1000mm peak to trough height. The calibration of such gauges is straightforward and stable.

3.2.2 Two-dimensional wave reflection

In a bounded fluid domain such as a wave tank or a wave flume, wave reflections from the boundaries of the basin are unavoidable. Moreover, the presence of a model in the tank will also lead to wave reflections. It is therefore important to work out the incident and reflected wave parameters.

An early method which can only be used with regular waves consists in placing two wave probes aligned with the direction of propagation of the waves and a quarter of the wavelength apart. While maintaining constant distance between the two probes, they are translated along the wave propagation direction until one is located at a node and the other one at an antinode of the standing wave pattern created by the reflection. This is easy to do if the gauges are properly calibrated and if a real-time signal proportional to the difference in wave heights at the two gauges is visibly displayed. Averaging the signal between the two probes yields the

incident wave amplitude. Dividing by two the difference between the two probes signal yields the reflected wave amplitude.

The above method is most practical in narrow wave tank. It is restricted to regular waves and prior knowledge of the wavelength is required. A large body of work on more versatile methods for 2-D wave reflection analysis is reported in the literature. This comes mainly from the field of coastal engineering.

Wave elevations are recorded simultaneously at a number of locations (at least two) in a line parallel to the direction of propagation of the waves, with a known spacing between the wave probes.

A Fourier transform is then applied to the time series to derive the different frequency components of the wave field. For each of these, the parameters of the incident and reflected waves are computed. When working with regular waves the Fourier transform is generally used to find out the fundamental frequency of the wave.

Various methods are then available to compute the incident and reflected wave parameters.

3.2.2.1 The Goda and Suzuki method

The earliest and simplest technique is described in Thornton and Calhoun (1972) and Goda and Suzuki (1976) and is often referred to as the Goda and Suzuki method. It involves only two measuring locations. For a regular wave, it assumes that the wave elevation measured at each probe is the sum of two sinusoids of the same frequency travelling in opposite directions. The method yields the amplitude of the incident and reflected waves as well as the phase shift between the two. Details on the implementation of the method can be found in Goda and Suzuki (1976) for random waves applications and in Isaacson (1991) for the case of regular waves. It is important to point out that the method exhibits singularities when the probe spacing is equal to an integer number of half wave lengths. It is therefore recommended to avoid the vicinity of the singularities. This is unfortunately not always possible when analysing reflections in random waves, especially with a wide spectrum range. A compromise needs therefore to be made which usually involves giving higher weightings to the frequency bands of interest, around the peak frequencies for example. More details on the range of application of this method can be found in the two previously cited references.

3.2.2.2 The Mansard and Funke method

The Mansard and Funke method (Mansard and Funke, 1980) is the most commonly used. It uses three wave probes and can be considered as an improvement of the Goda and Suzuki approach. As for the latter, sinusoids are fitted to the incident and reflected waves but the data from the extra probe makes it possible to minimise the squared error between the outcome of the fittings and the measured wave elevations. The main advantage of this method is to make the wave reflection analysis less sensitive to the noise contaminating the measurements (Isaacson, 1991). As with the previous approach, the Mansard and Funke method exhibits singularities. If the three probes are equidistant, the method breaks down when the spacing between two adjacent probes is an integer number of half wave lengths as for the previous method. If the

probes are not equidistant the conditions of occurrence of the singularities are more complex and can be found in Isaacson (1991) and Mansard and Funke (1980).

3.2.2.3 Discussion

In Isaacson (1991) the author presents a comparative study of the two above methods for regular waves. He carries out a sensitivity analysis on the accuracy of the incident and reflected wave parameters to errors on the measured wave elevations. The Mansard and Funke is found to be the most accurate.

It is important to point out that the two methods are based on linear dispersion theory. In other words, they assume that the incident and reflected waves are perfect sinusoids which is not the case in reality. This is illustrated in Mansard and Funke (1987) where the authors report that for regular waves, the incident and reflected wave heights estimated by their method are too small compared to the wave heights derived from zero crossing analysis. The process of fitting sinusoids to the wave field discards the bound harmonics from the analysis whereas the wave height computation relying on a zero crossing approach does not.

3.2.3 Multidirectional wave spectra

When analysing the performance of a wave energy converter model in a directional wave tank, it is important to estimate as accurately as possible the incident wave conditions to which the model is exposed.

Many techniques for deriving directional characteristics of wave fields are reported in the literature. Most of them were developed by oceanographers to measure waves in the real seas. Benoit et al. (1997) give a good overview of those different techniques and the present section will broadly follow this paper.

The dependency of the energy spectrum on frequency and direction is described by the energy spectrum $E(\omega, \theta)$ which is a function of the wave angular frequency ω and of the wave direction of propagation θ . E is an energy per unit sea surface, per unit frequency and per unit angle. The unit of E is therefore $\text{J.m}^{-2}.\text{Hz}^{-1}.\text{rad}^{-1}$ but is sometime expressed as $\text{N.m}^{-1}.\text{Hz}^{-1}.\text{rad}^{-1}$. It is also common to analyse a wave field in terms of directional variance spectrum $S(\omega, \theta)$. This corresponds to the variance of the wave elevation which is proportional to the wave energy:

$$S(\omega, \theta) = \frac{E(\omega, \theta)}{\rho g} \quad (3.6)$$

where ρ is the water density and g the gravitational acceleration. $S(\omega, \theta)$ is often referred to as the directional frequency spectrum and its unit is $\text{m}^2.\text{Hz}^{-1}.\text{rad}^{-1}$.

To illustrate the physical meaning of the directional frequency spectrum, it is useful to consider the wave field as a superposition of an infinite number of wave fronts of different frequencies

travelling in different directions. Assuming linearity, the wave elevation $\eta(x, y, t)$ at a point of spatial coordinates (x, y) at time t is given by:

$$\eta(x, y, t) = \sum_{n=1}^{\infty} a_n \cos(k_n(x \cos \theta_n + y \sin \theta_n) - \omega_n t + \phi_n) \quad (3.7)$$

where the a_n 's are the wave front amplitudes, the k_n 's the wave numbers, the θ_n 's the angles corresponding to the direction of propagation of the wave fronts, the ω_n 's the angular frequencies and the ϕ_n 's the phases. If the ϕ_n 's are distributed between 0 and 2π with a uniform probability density, $S(\omega, \theta)d\omega d\theta$ represents the contribution to the variance of the wave elevation due to wave components with frequencies between ω and $\omega + d\omega$ and directions between θ and $\theta + d\theta$:

$$S(\omega, \theta)d\omega d\theta = \sum_{\omega_n}^{\omega_n+d\omega} \sum_{\theta_n}^{\theta_n+d\theta} \frac{1}{2} a_n^2 \quad (3.8)$$

It is common practice to decompose the directional variance spectrum as follow:

$$S(\omega, \theta) = S(\omega)D(\omega, \theta) \quad (3.9)$$

where $S(\omega)$ is the 'non-directional' variance spectrum which is related to $S(\omega, \theta)$ by:

$$S(\omega) = \int_0^{2\pi} S(\omega, \theta) d\theta \quad (3.10)$$

and $D(\omega, \theta)$ is the Directional Spreading Function (DSF) which satisfies the two following properties:

$$D(\omega, \theta) \geq 0 \quad \text{for } \theta \in [0, 2\pi] \quad (3.11)$$

$$\int_0^{2\pi} D(\omega, \theta) d\theta = 1 \quad (3.12)$$

3.2.3.1 Estimation of the directional frequency spectrum

The estimation of the directional frequency spectrum requires the measurement of a set of quantities associated with the wave field. The most common quantity recorded in a wave tank is the surface elevation. Elevation at one point is not sufficient to derive directional information and one has to record it at at least three different locations to do so. The directional frequency spectrum can also be computed from a single point measurement, but in this case other quantities have to be recorded in addition to surface elevation. This technique is typically used in the real sea using a heave-pitch-roll buoy. The present document focuses on multi-point surface elevation since it is the most widely used technique in wave tanks. More information on the other methods can be found in Benoit et al. (1997).

Most methods for estimating the directional frequency spectrum rely on the relationship between the cross-spectra of the surface elevation at different points and $S(\omega, \theta)$. We will assume that M wave gauges are used to measure simultaneously the surface elevation at M different locations. The cross-spectra or cross-covariance spectral density between two surface elevation

signals η_p and η_q (from probes p and q with $p, q \leq M$ and $p \neq q$) is the Fourier transform of the cross-correlation between the two signals. Rigorous definitions of correlation and spectral density can be found in chapter 3 and 5 of Newland (2005) respectively. In the present context, the cross-correlation between η_p and η_q is defined by:

$$R_{pq}(\tau) = \lim_{T \rightarrow \infty} \frac{1}{T} \int_0^T \eta_p(t) \eta_q(t + \tau) dt \quad (3.13)$$

and the corresponding cross-spectra by:

$$G_{pq}(\omega) = \int_{-\infty}^{+\infty} R_{pq}(\tau) e^{-i\omega\tau} d\tau \quad (3.14)$$

Assuming linear wave theory and assuming that the phases of the different components of the wave field are randomly distributed the relationship between the directional frequency spectrum and the cross-spectra is as follow:

$$G_{pq}(\omega) = \int_0^{2\pi} e^{-ik \cdot (\mathbf{x}_q - \mathbf{x}_p)} S(\omega, \theta) d\theta \quad \text{for } p = 1, \dots, M \quad \text{with } p < q \quad (3.15)$$

The vector \mathbf{k} is the wave number vector defined by:

$$\mathbf{k} = \begin{pmatrix} k \cos \theta \\ k \sin \theta \end{pmatrix} \quad (3.16)$$

\mathbf{x}_p and \mathbf{x}_q are the vectors corresponding to the location of wave gauge p and q respectively. It should be noted that (3.15) is more complex when the quantities measured at point p and q are different from surface elevation. More details on that topic can be found in Benoit et al. (1997).

Estimating the directional frequency spectrum involves computing the cross-spectra (3.14) from all the pairs of wave gauges and then invert the relationship given by (3.15). The later operation is the most complex and tedious. With an infinite number of wave gauges, $S(\omega, \theta)$ can be in principle determined uniquely. In practice, there is only a finite number of probes (typically five to seven) and so the mathematical problem is not fully defined. Consequently some assumptions on $S(\omega, \theta)$ are required to yield a unique solution.

Several practical methods are available for estimating the directional frequency spectrum. None of them is perfect, they all have pros and cons. This document will briefly present and discuss the two most widely used. A more extensive review of the available methods can be found in Benoit et al. (1997).

3.2.3.2 The maximum likelihood method

The Maximum Likelihood Method (MLM) was originally introduced by Capon et al. (1967) in the field of seismic wave detection. The MLM relies on the assumption that the estimate of the directional frequency spectrum $\tilde{S}(\omega, \theta)$ can be expressed as a linear combination of the

cross-spectra between the surface elevation measurements:

$$\tilde{S}(\omega, \theta) = \sum_{p=1}^M \sum_{q=1}^M \alpha_{pq}(\omega, \theta) G_{pq}(\omega) \quad (3.17)$$

Expressing $G_{pq}(\omega)$ from (3.15) yields:

$$\tilde{S}(\omega, \theta) = \sum_{p=1}^M \sum_{q=1}^M \alpha_{pq}(\omega, \theta) \int_0^{2\pi} e^{-i\mathbf{k}' \cdot (\mathbf{x}_q - \mathbf{x}_p)} S(\omega, \theta') d\theta' \quad (3.18)$$

where

$$\mathbf{k}' = \begin{pmatrix} k \cos \theta' \\ k \sin \theta' \end{pmatrix} \quad (3.19)$$

(3.18) can be rewritten as:

$$\tilde{S}(\omega, \theta) = \int_0^{2\pi} w(\omega, \theta, \theta') S(\omega, \theta') d\theta' \quad (3.20)$$

where

$$w(\omega, \theta, \theta') = \sum_{p=1}^M \sum_{q=1}^M \alpha_{pq}(\omega, \theta) e^{-i\mathbf{k}' \cdot (\mathbf{x}_q - \mathbf{x}_p)} \quad (3.21)$$

In (3.20), $\tilde{S}(\omega, \theta)$ can be seen as expressed as the convolution product of the true directional frequency spectrum by the window function $w(\omega, \theta, \theta')$. The more $w(\omega, \theta, \theta')$ tends toward a Dirac function, the better estimate $\tilde{S}(\omega, \theta)$ is of $S(\omega, \theta)$. Isobe and Kondo (1984) have shown that this is best achieved when:

$$\tilde{S}(\omega, \theta) = \frac{\kappa}{\sum_{p=1}^M \sum_{q=1}^M G_{pq}^{-1}(\omega)} \quad (3.22)$$

where the $G_{pq}^{-1}(\omega)$ stands for the elements of the inverse of the cross-spectral matrix. The factor κ is derived by ensuring that the integral of $\tilde{S}(\omega, \theta)$ over the $[0, 2\pi]$ interval is equal to the measured non-directional variance spectrum (see equations (3.9) and (3.10)):

$$\int_0^{2\pi} \tilde{S}(\omega, \theta) d\theta = S_{measured}(\omega) \quad (3.23)$$

The MLM is often considered as one of the best methods for estimating the directional frequency spectrum and it is widely used. Benoit and Teisson (1994) have shown however that this method tends to overestimate the width of the directional peaks of the true spectrum.

It should be mentioned that the MLM does not perform as well in the presence of reflected waves. This is because reflection introduces phase locking (see section 4.4 p.40) which means that the phase of the different wave components forming the wave field are no longer randomly distributed. More details on the MLM performance with reflected waves can be found

in Davidson et al. (1998).

3.2.3.3 The Bayesian directional method

The Bayesian Directional Method (BDM) relies on the Bayesian probability technique to estimate the directional frequency spectrum. The Bayesian approach was first introduced to wave directionality analysis by Hashimoto and Kobune (1988). It has the advantage that it does not require any assumption on the shape of the Directional Spreading Function (DSF) except that it can be expressed as a piecewise constant function. It also accounts for potential errors in the cross-spectra computation.

The interval of definition $[0, 2\pi]$ of the DSF is divided into K subintervals of equal width $\Delta\theta$ over which the estimate of the DSF $\tilde{D}(\omega, \theta)$ is assumed to be constant. A series $x_k(\omega)$ of K elements ($k = 1, \dots, K$) is defined:

$$x_k(\omega) = \ln D(\omega, \theta_k) \quad \text{where} \quad \theta_k = \left(k - \frac{1}{2}\right) \Delta\theta \quad (3.24)$$

from which the DSF can be approximated as follows:

$$\tilde{D}(\omega, \theta) = \sum_{k=1}^K I_k(\theta) e^{x_k(\omega)} \quad \text{where} \quad I_k(\theta) = \begin{cases} 1 & \text{when } (k-1)\Delta\theta \leq \theta \leq k\Delta\theta \\ 0 & \text{otherwise} \end{cases} \quad (3.25)$$

(3.25) is then inserted into (3.15) to yield a system of non-linear equations. The Bayesian method also includes a smoothness condition on the directional frequency spectrum function which consists in minimising the following quantity:

$$\sum_{k=3}^K (x_k - 2x_{k-1} + x_{k-2})^2 \quad (3.26)$$

The detailed derivation of the Bayesian directional method is complex and can be found in Hashimoto and Kobune (1988).

The BDM is very versatile and reliable and is therefore widely used. As for the MLM, it does not perform as well in the presence of reflected waves. More information on this topic can be found in Ilic et al. (2000); Chadwick et al. (2000).

3.3 Wave height and period parameters

The parameters characterising regular waves are straightforward and the only possible confusion is whether the wave is described in terms of amplitude or height (the height being twice the amplitude). Things are however more complicated when it comes to spectral seas. A range of parameters have been devised to describe those. Different professions, ranging from early mariners to oceanographers and to wave energy researchers have come up with different param-

eters, often reflecting the measurement and analysis techniques they are using. The following section will give a brief overview of those. A more comprehensive list can be found in IAHR (1987). Further detail on the derivation of some of the parameters can be found in Tucker and Pitt (2001).

3.3.1 Height parameters

The most commonly known, particularly amongst oceanographer, wave height parameter is the ‘significant wave height’ often noted H_{sig} , H_s or $H_{1/3}$. It is defined as the average of the highest one-third of the wave heights. Such a definition might sound confusing but it was motivated by the fact that H_{sig} could be assessed by mariners without any instrument. An observer would climb to a point in a ship from where one in three waves appears to come above the horizon. The level of the observer’s eyes above the still water line of the ship was the significant wave height. From the time series of a wave record, H_{sig} is calculated from zero-crossing wave heights. The zero upcrossing/downcrossing wave height is the range of wave elevation between two zero upcrossings/downcrossings of the mean water level. These are noted H_u and H_d respectively and are illustrated by figure 3.6 which shows a wave record time series.

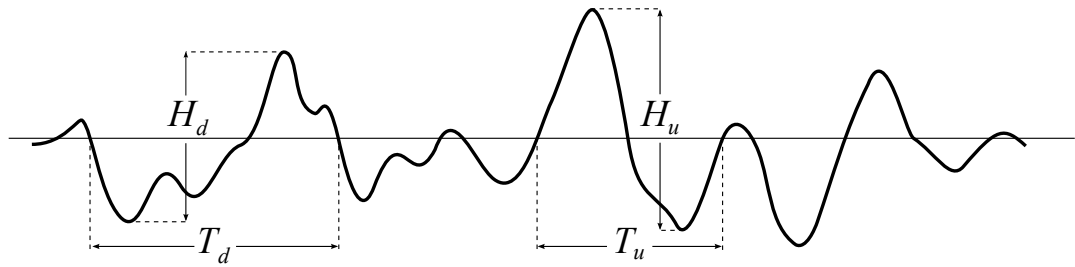


Figure 3.6: Wave record time series where H_u and T_u are the zero upcrossing wave height and period respectively and H_d and T_d are the zero downcrossing wave height and period respectively.

With modern digitisation of wave records, frequency analysis became possible and is now common practice. The significant wave height estimated using this method is noted H_{m_0} . It is derived from the zeroth moment of the non-directional variance spectrum $S(f)$:

$$H_{m_0} = 4\sqrt{m_0} \tag{3.27}$$

At that stage it might be useful to introduce the concept of spectral moments as these are used in the definition of several statistical wave parameters. The n^{th} spectral moment is defined as:

$$m_n = \int_0^\infty f^n S(f) df \tag{3.28}$$

In particular,

$$m_0 = \int_0^\infty S(f) df \tag{3.29}$$

Coming back to the significant wave height parameter, it should be noted that H_{m_0} is usually not exactly equal to H_{sig} computed from time domain analysis. To avoid any confusion, the significant wave height computed from frequency analysis should always be noted H_{m_0} .

In the early days of wave power research, the Wave Power Group of the University of Edinburgh preferred a parameter based on Root Mean Square (RMS) calculation. Every measurement of the wave record time series is squared, then the mean of all the squared measurements is calculated and the final stage is to take the square root of the mean. As reported by Jeffrey et al. (1978), RMS “comes into lots of calculations of power and energy, gets over difficulties with negative numbers and pays more attention to the extreme values in a record.” This parameter was originally noted H_{rms} which can be confusing given that it actually corresponds to the RMS of the wave elevation. It should be noted that:

$$H_{m_0} = 4H_{rms} \quad (3.30)$$

3.3.2 Period parameters

Historically, wave records were only analysed in the time domain and a popular period parameter was the mean of the zero upcrossing or downcrossing periods noted respectively $\overline{T_u}$ and $\overline{T_d}$ (IAHR, 1987). The zero upcrossing period is often noted T_u and the zero downcrossing T_d . Their meaning is illustrated on figure 3.6. Another common notation for $\overline{T_u}$ is T_z (Tucker and Pitt, 2001).

For a regular wave of period T , the total power available per unit of wave crest (power density) is given by:

$$P = \frac{\rho g^2}{4\pi} H_{rms}^2 T = \frac{\rho g^2}{64\pi} H_{m_0}^2 T \quad (3.31)$$

where ρ is the water density, g the gravitational acceleration. Now considering a spectral sea where at a given location, the power density P and the wave height parameters are known, then the energy period T_E is defined by:

$$P = \frac{\rho g^2}{4\pi} H_{rms}^2 T_E = \frac{\rho g^2}{64\pi} H_{m_0}^2 T_E \quad (3.32)$$

So conceptually, the energy period of a given spectrum corresponds to the period of a regular wave which would have the same significant wave height H_{m_0} and the same energy content as that spectrum.

T_E can be expressed in terms of spectral moments (see equation (3.28)):

$$T_E = \frac{m_{-1}}{m_0} \quad (3.33)$$

Another widespread period parameter is the ‘peak period’ noted T_p which corresponds to the period for which the non-directional variance spectrum is maximum. T_p cannot be calculated

exactly from spectral moments. However, a good approximation, noted T_{pc} , is given by:

$$T_{pc} = \frac{m_{-2}m_1}{m_0^2} \quad (3.34)$$

3.3.3 Time domain versus frequency domain parameters

In the early days, wave elevation measurements were recorded graphically on paper charts. Analysis of these records was carried out by hand and mainly based on the zero crossing method. With the improvement of wave measurement technology it has become possible to carry out frequency analysis of the records. Time domain analysis (based on the zero crossing method) is however still in use.

A major drawback of the zero crossing method is that its outcome is strongly affected by the frequency bandwidth of the measuring equipment. This is illustrated in figure 3.7 showing numerical simulations of two records of the same sea state measured with different bandwidths. On the left records, high frequency components are filtered out whereas it is not the case on the right record. It can be seen that the quantities derived from zero crossing will be different for both records.

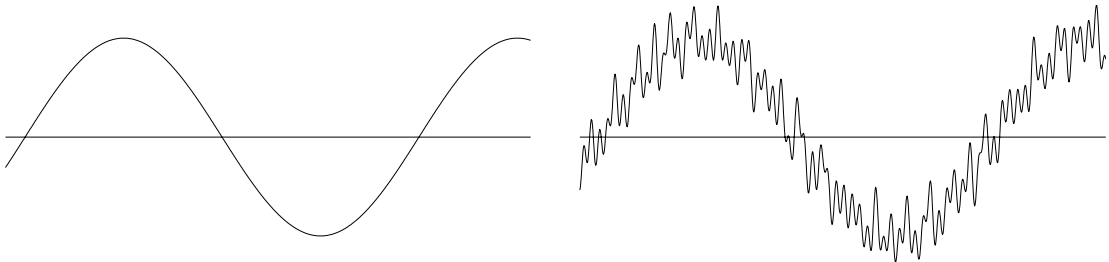


Figure 3.7: Numerical simulations of two records of the same sea state. On the left record, the high frequency components are filtered out. The record on the right is not filtered.

In the field of wave energy, frequency analysis is more widespread than time domain, especially for spectral seas. It should be noted however that time domain analysis may account better for some of the non-linearities of the wave field. This is due to the linear techniques associated with the Fourier analysis. As an example, the information on the asymmetry of the wave profile is lost through the sine correlations associated with the Fourier analysis.

3.4 Video motion tracking device

A video motion tracking device provides real time displacement information for the six degrees of freedom (surge, sway, heave, roll, pitch and yaw) of the model without mechanically interfering with it. An increasing number of research institutions have equipped their wave tank with such system. The leading manufacturer is Qualisys AB.

3.4.1 System description

The measurement technique relies on the principle of triangulation. Several infrared-sensitive cameras (at least two) are set to view the area where the model moves. The measurement volume is defined by the overlap of the respective camera fields of view. The cameras detect the position of small markers attached to the model. Two-dimensional position data from each camera are processed, together with information about camera locations, to compute the three-dimensional co-ordinates of the markers.

In order to compute motions of a rigid body in terms of the classic six degrees of freedom, more than one marker is necessary. The different markers have to be fitted on the model in a way that ensures that their position relative to each others is constant. This way, position and orientation data relative to this 'network' of markers can be computed in a local coordinate system.

The markers can be either active infra-red emitting devices or passive reflectors. The advantage of active markers is that they can be 'seen' accurately by the cameras from further away than with passive ones. Passive markers reflect flashes emitted by the array of infra-red LEDs located around the lens on the front of each camera. They typically consist of hollow plastic spheres coated with a retro-reflective material. The cameras work out the position of the centroid of those markers, which means that there is no direct relation between the radius of the spheres and the accuracy of the measurement.

The spatial resolution of the system is directly related to the size of the field of view. This is because the cameras are capable of determining a marker's position with an accuracy which corresponds to a fixed proportion of each camera's sensor area. In other words, operating with a larger measurement volume will yield poorer accuracy and vice versa.

3.4.2 User guidance

The manuals of Qualysis systems are very complete but it might be useful to recall few recommendations.

3.4.2.1 Marker size

Passive markers come in various sizes, typically ranging from 7 to 40 mm in diameter. Smaller markers are often easier to attach to models and because they are less cumbersome, they are less likely to overshadow other markers from the cameras. One has however to make sure that the size of the markers as seen by the cameras is large enough. With a Qualysis system, these numbers are shown for each camera on the 2D data info window. The marker sizes are given in terms of angle of the field of view of the camera and along the x and y axes of the camera sensor. For a given camera optic, the marker size as seen by the camera will depend on the actual physical size of the marker, its distance to the camera and the lens used. Qualysis recommends a minimum size of 7 units.

3.4.2.2 Marker reflection

When using a Qualisys system in a wave tank, it is very likely that for some of the markers, both the actual marker and its reflection on the water surface will be in the field of view of a camera. This can create spurious marker traces especially when the water surface is still. To address this issue, the best is to implement marker discrimination. This functionality allows to set a threshold on the size of the markers as seen by the camera. In other words, all the traces whose size are under the threshold are discarded. Given that traces of reflected markers are less 'bright' than the actual markers, this technique works quite well. It should be made sure however that all the physical size of the true markers are suitably chosen so that the discrimination does not discard a true marker. This could be the case with a model where all the markers have the same diameter but some are further away from the cameras than others. The traces due to reflection of the close ones could be of the same size as the trace of true most remote markers.

3.4.2.3 Rigid body considerations

In order to record the motion of a model along the six rigid degrees of freedom (surge, sway, heave, pitch, roll and yaw), it is necessary to fit the model with at least four markers whose positions with respect to each other are fixed. The markers must not lie on the same horizontal plan. Ideally the distances between any two markers of the rigid body should be unique i.e. different from the distance between any other combination of two markers. This is illustrated in figure 3.8 where four markers (A, B, C and D) are laid out suitably. As an example, the distance AB differs from the distances, BC, CD, AD, AC, and BD.

Qualisys recommends that those distances differ by at least a margin they call 'bone length tolerance'. This is to ensure that when computing the position of the rigid body, a given segment (or bone) connecting two markers cannot be mistaken with another one of similar length.

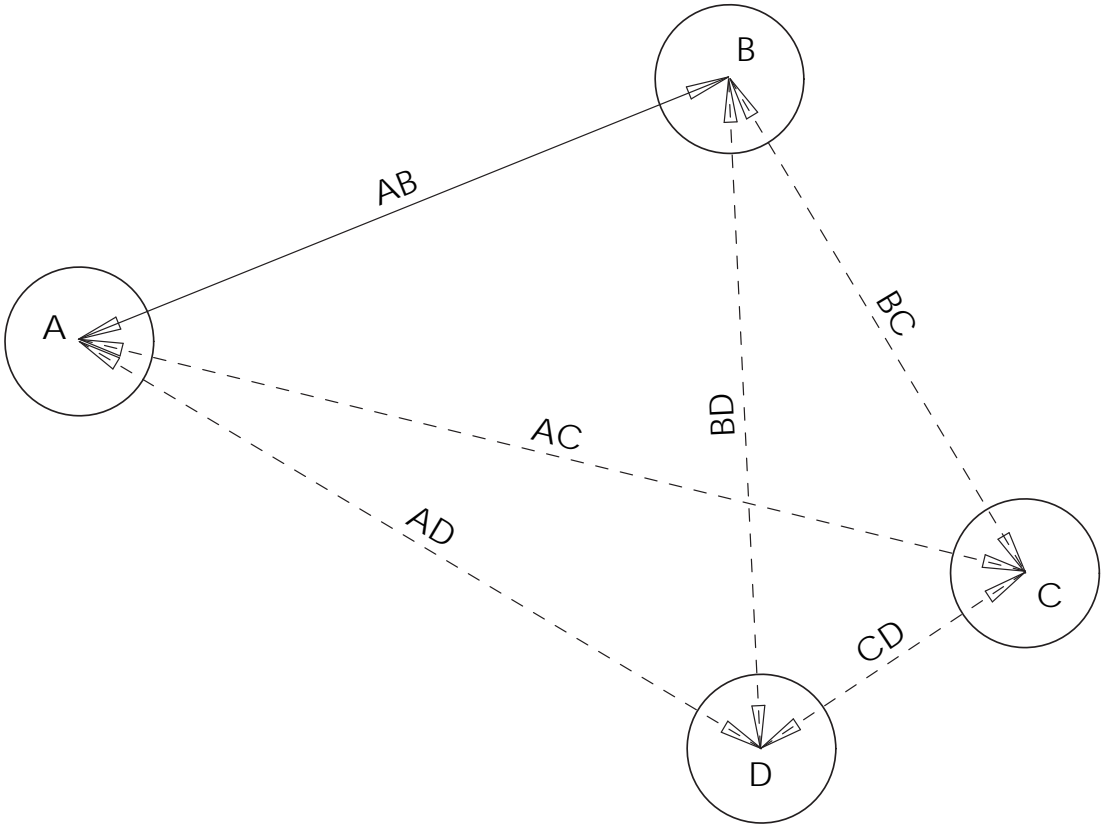


Figure 3.8: *Marker positioning considerations*

Wave generation

Two main classes of wave field are commonly generated in wave tanks: regular and irregular waves. The former type is simpler in that it is theoretically only associated with a limited number of parameters, namely one frequency and one amplitude. Tank testing of WECs in regular waves is very useful, especially in the early design stage. It helps gaining a qualitative and quantitative understanding of the behaviour of the device in a environment controlled by only a few parameters. Regular waves are however virtually never encountered in the ocean and it is therefore important to also test WEC models in more ‘realistic’ irregular waves.

To create irregular waves in a wave basin, an appropriate command signal needs to be sent to the wave-makers control system. The derivation of the command signal is basically done in two stages.

- A wave elevation time series corresponding to the desired target sea state (or spectrum) is computed.
- The wave tank ‘transfer function’ is used to convert the above times series into the command signal.

The transfer function is the relation between the signal sent to the wave maker and the corresponding wave generated. Each wave basin has its own specific transfer function which depends on its geometry and on the wave-makers geometry, dynamics and drive system.

In most wave basins, the wave elevation time series is actually discrete and obtained by Inverse Discrete Fourier Transform (IDFT). The time series is computed by IDFT from the DFT complex coefficients (see equations (3.3) and (3.4) p.18) which correspond to a target spectrum. The DFT coefficients can be derived according to different methods as will be explained in the following sections.

There are mainly two approaches to irregular wave generation. They are referred to as ‘deterministic’ and ‘non-deterministic’ or ‘probabilistic’. The debate on which of these is better is perhaps more philosophical than technical and to this day, there is still no widely acknowledged consensus on the topic. The author will not venture in addressing the debate but will just state the main advantages and disadvantages of each ‘school of thought’. More arguments for this debate can be found in Funke and Mansard (1987) and Huntington (1987).

4.1 The deterministic approach

4.1.1 Random phase method

This method is based on the IDFT. The amplitude of the DFT coefficients are computed from the target spectrum so that they are proportional to the square root of the desired spectral density. The phase for each coefficient is chosen randomly. The random generation of the phase values is however initiated by a 'seed' so that the series of phase values can be repeated identically at will by keeping the same seed number. The time series output from the IDFT is thus fully defined by the target spectrum and the seed number. This wave generation process is therefore considered deterministic. The length of the time series is often called the 'repeat period' or 'recycling length' of the command signal. More information on this method and its implementation can be found in Tuah and Hudspeth (1982).

4.1.2 Pros and cons of the deterministic approach

The main advantage of this method is that the discretised target spectrum can be guaranteed over the 'repeat period'. This allows reasonably short wave basin run times compared with the deterministic approach. The repeatability of wave trains generated is also an advantage when carrying out comparative studies. The drawback of the deterministic approach is that it does not reproduce the true random behaviour of ocean waves. When using relatively short repeat periods, this can lead to 'missing' some extreme events of low probability in the real world. The advocates of the deterministic approach argue that this issue can be overcome by generating extreme events separately in a deterministic manner. The supporters of the probabilistic method point out that such techniques imply assumptions by the experimenter of what an extreme event is. It is possible that phenomena other than large amplitude waves might generate extreme events for the wave power device studied. These could be for example a specific wave groupiness which, combined with the device dynamics leads to an extreme response. Such an extreme event would be difficult to predict.

4.2 The non-deterministic approach

4.2.1 Random complex spectrum method

As for the random phase method, the random complex spectrum method relies on the IDFT. The complex DFT coefficients are computed from a target spectrum. They are obtained by multiplying the square root of the desired spectral density values by a random variable having a Gaussian distribution with zero mean and standard deviation of 1. This can be considered as 'filtering' the random variable by the square root of the desired spectral density. More information on this method and its implementation can be found in Tuah and Hudspeth (1982).

4.2.2 White noise filtering method

The white noise filtering method consists in convoluting (or ‘filtering’) a synthesised random number sequence (i.e. a white noise signal) with spectral values from the desired target spectrum. Applying the IDFT to the target spectrum yields the corresponding discrete time series. This time series can be considered as the coefficients of a digital filter which is then applied to the white noise time series. The outcome is the command signal for the wave-maker control system. More on this method can be found in Bryden and Greated (1984).

The term ‘white noise’ comes from the analogy with white light, whose spectrum is approximately constant over the range of visible frequency. The term noise comes from the field of electronics. White noise refers to a signal whose energy is evenly spread over the spectrum of interest.

4.2.3 Pros and cons of the non-deterministic approach

The realisation of a sea state using this method will only match the target spectrum within the bounds of probability. In other words, the exact realisation of the target spectrum is only guaranteed for runs of infinite duration. From a practical point of view, this means that experimental runs have to be rather long to properly represent the target spectrum. As an example, spectral shape for typical 20 minute realisations can deviate very significantly from the target spectrum (Miles and Funke, 1989).

All the realisations of a same target spectrum will be different, although statistically similar. This might not be appropriate for comparing the performance of different devices under similar sea states. On the other hand, the spectral shape obtained will have similar statistical variability to that of real ocean waves over the same duration.

4.3 Wave tank calibration

A wave tank transfer function ‘translates’ the wave elevation command signal to the wave-makers into physical wave heights in the basin. The theoretical derivation of such transfer functions was pioneered by Biésel and Suquet (1951) for piston and flap type wave-makers controlled in displacement.

When working with regular waves, the quantities investigated are often ‘normalised’ by the measured wave height. This approach tends to limit the impact of inaccuracies in the transfer function in the sense that even if the height of the generated waves is slightly different from the target height, at least, the actual wave height is known and taken into account through the ‘normalisation’ process. The accuracy of the transfer function is however particularly important when working with irregular waves. If for some frequencies, the height of the waves generated does not correspond to the target height, the actual energy spectrum will be distorted compared to the target one.

If a theoretically derived transfer function is a good starting point it is recommended to refine it through experimental wave tank calibration.

As an example, with Edinburgh Design Ltd. wave making systems, the tank transfer function file requires specifying gain values for discrete wave frequencies and discrete wave heading angles (Rogers and Bolton King, 1997). The gain relates the target wave height with the voltage of the command signal for the wave frequency and heading angle considered. The more gain values are specified, the better the transfer function. Covering the whole frequency spectrum and angle range with a fine resolution can however prove long and tedious. It is therefore possible to only specify a limited number of gain values and let the wave-maker control system interpolate between these.

When carrying out the calibration, it is recommended to process the wave elevation time series recorded using a wave reflection analysis technique. Since only a single direction of wave propagation is considered at a time, a two dimensional method is generally considered sufficient (see section 3.2.2 p.24).

The gain is generally linearly related to the height of the waves generated. Calibration for a single frequency and angle can therefore be achieved with a single set of measurements by adjusting the gain linearly with the error between the target wave height and the measured value. To achieve a more accurate calibration, an iterative method can be adopted.

Figure 4.1 shows the measured energy spectra for a long crested modified Pierson Moskowitz sea generated in the Edinburgh Curved tank before (a) and after (b) calibration. Measurements have been carried out by Jorge Lucas. He has used the two dimensional Mansard and Funke reflection analysis method (see section 3.2.2 p.24) to separate the incident from the reflected waves. The improvement brought about by the calibration is very significant.

4.4 Phase locking

4.4.1 General considerations

Phase locking is a phenomenon happening when regular waves of equal frequency and with constant phase shift between each other are superposed. The direction of propagation of these waves can be different. The resulting wave field is affected by patterns of nodes and antinodes which makes it spatially inhomogeneous and non-ergodic. This means among other things that the statistical properties of quantities linearly associated with this wave field will be different from one point of the wave field to another. More detail on the impact of non-ergodicity and inhomogeneity can be found in Jefferys (1987).

The simplest example of phase locking can be observed when a regular wave hits perpendicu-

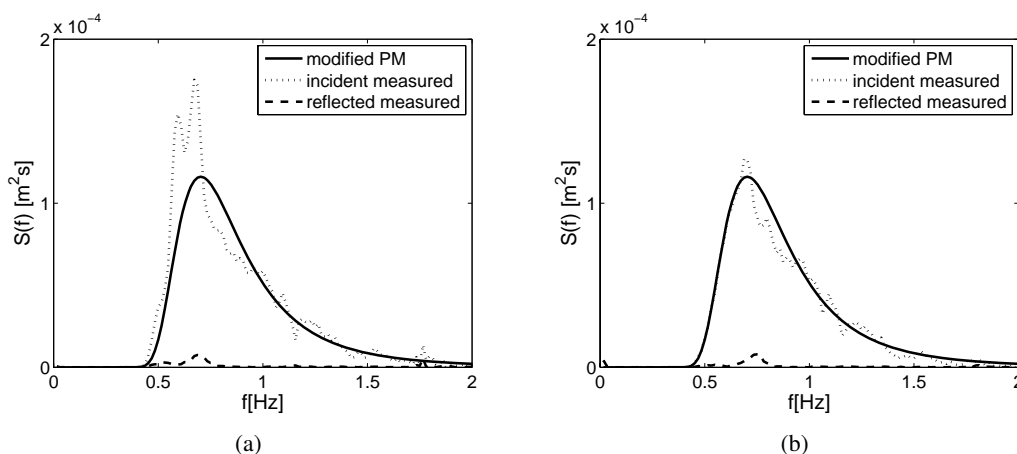


Figure 4.1: Realisations of a modified Pierson Moskowitz spectrum before (a) and after (b) wave tank calibration. The solid line corresponds to the target spectrum, the dotted line to the incident measured spectrum and the dashed line to the reflected measured spectrum.

larly a fully reflective vertical wall. A reflected wave of equal frequency and amplitude travelling in the opposite direction forms. The phases of the incident and reflected waves are locked by the fact that they are both equal on the wall. The resulting wave pattern is that of a standing wave with nodes and antinodes. When measuring the wave height of a standing wave, the value obtained will be strongly affected by the spatial location at which the measurement is taken. At a node, the wave height will almost be zero whereas at an antinode it will be maximum (about twice the height of the incident regular wave).

Phase locking is an important phenomenon to be aware of when carrying out model testing in a wave tank. Wave basins are by nature bounded fluid domains and no beach or wave-maker has perfect absorption characteristics. The wave field generated in the tank will be inevitably affected by reflections and thus phase locking. The scale of the non-ergodicity and spatial inhomogeneity due to wave reflection depends on many parameters including tank geometry, presence of reflecting side walls, reflection characteristics of the beach at the wave frequency considered, the heading angles of the wave generated. It is therefore advisable to ‘map’ the tank to find out which parts of it are the least affected by reflection for given wave conditions and therefore the most suitable to locate the model to be investigated. Before model testing, it is also recommended to measure the waves in the absence of the model at the location where the model is to be placed to ensure that they correspond to the target wave conditions.

Lack of spatial homogeneity can have a significant impact when investigating the behaviour of a free-floating wave energy device in a wave basin, especially if the mooring is compliant. Drift force and low frequency mooring oscillations can move the model away from its original position and if the wave field is not homogenous ‘enough’, the model might end up being subjected to waves whose characteristics are different from those of the waves recorded at the original location of the model.

4.4.2 Wave generation considerations

When generating multi-directional irregular seas, phase locking can be an issue. This depends on which generation technique is used.

4.4.2.1 Double summation method

The double summation method was originally the most commonly used approach for generating multi-directional spectra. With this technique, the target wave height η is defined as follows:

$$\eta(x, y, t) = \sum_{i=1}^N \sum_{j=1}^M A_{ij} \cos(\omega_i - k_i(x \cos \theta_j + y \sin \theta_j) + \phi_{ij}) \quad (4.1)$$

where x and y are horizontal spacial coordinates, t is time, the A_{ij} 's are the amplitudes of the wave components, the ω_i 's are the discrete radian frequencies of the wave components, the k_i 's are the corresponding wave numbers, the θ_j 's are the heading angles of the wave components and the ϕ_{ij} 's are the phases.

From equations (4.1) the target spectrum is made of $N \times M$ wave fronts spread over N discrete frequencies and M discrete angles. The main limitation of this method lies in the fact that for each frequency ω_i there are M wave fronts of different direction with exactly that same frequency. This leads to phase locking. The resulting spatial inhomogeneity can be significant. Jefferys (1987) carried out numerical simulation of a $\cos^2 \theta$ directional sea with 36 phase locked wave components. He found that over an area of one square kilometre, the mean energy at 0.1Hz computed from wave elevation varies between zero and four times the spatial mean value.

There are ways to improve the ergodicity and the spatial homogeneity of the double summation method. Miles and Funke (1989) present a method which consists in increasing the number of discrete frequencies in the spectrum definition given by (4.1). Instead of expressing each frequency bin of the target spectrum by a single frequency component, the bins are represented by P frequency components each. These frequencies ω_{iq} are defined as follows:

$$\omega_{iq} = \left(\omega_i - \frac{\Delta\omega}{2} \right) + q \frac{\Delta\omega}{P} \quad \text{for } q = 1, \dots, P \quad (4.2)$$

where ω_i is the same as in (4.1) and $\Delta\omega$ is the width of the bin.

Miles and Funke (1989) have then numerically investigated the variability of the variance of wave elevation η and of the cross-spectra. They have found that ergodicity and homogeneity can be improved by increasing the value of P but this also increases the computational burden involved. They also point out that the length of the record used to compute the cross-spectra has a significant impact on the variability. Variability can also be reduced by ensemble averaging over several realisations (Jefferys, 1987).

4.4.2.2 Single summation method

A multi-directional irregular sea-state generated by the single summation method has only one wave component at any particular frequency. The target wave height η is defined as follows (Miles and Funke, 1989):

$$\eta(x, y, t) = \sum_{i=1}^{N \times M} A_i \cos(\omega_i - k_i(x \cos \theta_i + y \sin \theta_i) + \phi_i) \quad (4.3)$$

where $\omega_i = i \frac{\Delta\omega}{M}$ with M being the number of heading angles. The θ_i 's are defined so that all the M heading angles are included in each frequency bin of width $\Delta\omega$. In other words, each bin of width $\Delta\omega$ is split into M equally wide segments with a single wave component per segment. The M wave components of a bin correspond to the M heading angles and they all have slightly different frequencies.

With all the wave components having different frequencies, there is no phase locking and the sea state generated is spatial homogenous and ergodic. The quality of the waves generated with this method will improve with increasing M and decreasing $\Delta\omega$ but values of these parameters can be limited by the angular and frequency resolutions of the wave-making system. Miles and Funke (1989) carried out numerical simulation and found out that the derivation of the cross spectra will be 'reasonably accurate' with $M = 32$ and $\Delta f = 0.04\text{Hz}$ with $\Delta f = \frac{\Delta\omega}{2\pi}$. Miles and Funke (1989) point out that the maximum wave heights in sea states generated with this method may tend to be smaller than those of a corresponding realisation in a real sea.

References

- Benoit, M., Frigaard, P., and Schäffer, H. A. (1997), Analysing multidirectional wave spectra: A tentative classification of available methods, in *IAHR Seminar on Multidirectional Waves and their Interaction with Structures*, pp. 131–158, San Francisco, US.
- Benoit, M. and Teisson, C. (1994), Laboratory comparison of directional wave measurement systems and analysis techniques, in *Proceedings of the 24th International Conference on Coastal Engineering*, pp. 42–56, Kobe, Japan.
- Biéssel, F. and Suquet, F. (1951), Les appareils générateurs de houle en laboratoire, *La Houille Blanche*, 6(2), pp. 147–165.
- Bryden, I. G. and Greated, C. A. (1984), Generation of three-dimensional random waves., *Journal of Physics D: Applied Physics*, 17(12), pp. 2351 – 2366.
- Capon, J., Greenfield, R., and Kolker, R. (1967), Multidimensional maximum-likelihood processing of large aperture seismic array, *IEEE Proceedings*, 55(2), pp. 192–211.
- Chadwick, A., Ilic, S., and Helm-Petersen, J. (2000), Evaluation of directional analysis techniques for multidirectional, partially reflected waves. part 2: Application to field data, *Journal of Hydraulic Research*, 38(4), pp. 253–258.
- Clayson, C. (1989), Survey of instrumental methods for the determination of high-frequency wave spectrum, Technical Report 267, Institute of Oceanographic Sciences Deacon Laboratory.
URL <http://eprints.soton.ac.uk/15285/01/267.PDF>
- Cooley, J. and Tukey, J. (1965), An algorithm for the machine calculation of complex Fourier series', *Mathematics of Computation*, 19, pp. 297–301.
- Davidson, M. A., Huntley, D. A., and Bird, P. A. (1998), Practical method for the estimation of directional wave spectra in reflective wave fields, *Coastal Engineering*, 33(2-3), pp. 91–116.
- Funke, E. and Mansard, E. (1987), A rationale for the use of the deterministic approach to laboratory wave generation, in *IAHR Seminar on WAVE ANALYSIS AND GENERATION IN LABORATORY BASINS*, pp. 153–195, Lausanne, Switzerland.
- Goda, Y. and Suzuki, Y. (1976), Estimation of incident and reflected waves in random wave experiments, in *15th Coastal Engineering Conference*, pp. 828–845.
- Hashimoto, N. and Kobune, K. (1988), Directional spectrum estimation from a bayesian approach, in *21st Coastal Engineering Conference*, pp. 62–76, Malaga, Spain.
- Huntington, S. (1987), A rationale for the use of the probabilistic approach to laboratory wave generation, in *IAHR Seminar on WAVE ANALYSIS AND GENERATION IN LABORATORY BASINS*, pp. 197–208, Lausanne, Switzerland.

- IAHR (1987), List of sea state parameters, in *IAHR Seminar on WAVE ANALYSIS AND GENERATION IN LABORATORY BASINS*, pp. 17–48, Lausanne, Switzerland.
- Ilic, S., Chadwick, A., and Helm-Petersen, J. (2000), Evaluation of directional analysis techniques for multidirectional, partially reflected waves. part 1: Numerical investigations, *Journal of Hydraulic Research*, 38(4), pp. 243–251.
- Isaacson, M. (1991), Measurement of regular wave reflection, *Journal of Waterway, Port, Coastal and Ocean Engineering*, 117(6), pp. 553–569.
- Isobe, M. and Kondo, K. (1984), Method for estimating directional wave spectrum in incident and reflected wave field, in *Proceedings of the 19th International Conference on Coastal Engineering*, pp. 467–483.
- Jefferys, E. R. (1987), Directional seas should be ergodic, *Applied Ocean Research*, 9(4), pp. 186–191.
- Jeffrey, D., Keller, G., Mollison, D., Richmond, D., Salter, S., Taylor, J., and Young, I. (1978), 4th year report on Edinburgh Wave Power Project, Study of Mechanisms for Extracting Power from Sea Waves, Technical Report 1, The University of Edinburgh, Scotland.
URL www.see.ed.ac.uk/~ies/Wave_power_group_reports/4TH_YEAR_REPORT_STUDYING_MECHANISMS_FOR_EXTRACTING_POWER_FROM_SEA_WAVES.pdf
- Jeffrey, D. C., Richmond, D. J. E., Salter, S. H., and Taylor, J. R. M. (1976), Study of mechanisms for extracting power from sea waves, Technical report, University of Edinburgh.
URL www.see.ed.ac.uk/~ies/Wave_power_group_reports/EWPP%202nd%20year%20report%20OCR%20reduced%20plus%20photos.pdf
- Liaw, C. (1994), Dynamic Instability of a Parametric Excited Ship Rolling Model, *International Journal of Offshore and Polar Engineering*, 4(2), pp. 105–111.
- Lucas, J., Cruz, J., Salter, S., Taylor, J. R. M., and Bryden, I. G. (2007), Update on the modelling of a 1:33 scale model of a modified Edinburgh duck wec, in *7th European Wave and Tidal Energy Conference*, Porto, Portugal.
- Mansard, E. P. D. and Funke, E. R. (1980), Measurement of incident and reflected spectra using a least squares method, in *17th International Conference on Coastal Engineering*, pp. 95–96, Sydney, Australia.
- Mansard, E. P. D. and Funke, E. R. (1987), Experimental and analytical techniques in wave dynamics, a comparative study, in *IAHR Seminar on WAVE ANALYSIS AND GENERATION IN LABORATORY BASINS*, pp. 91–116, Lausanne, Switzerland.
- Maunsell, C. and Murphy, T. (2005), Effects of air compressibility in Oscillating Water Column Physical Modelling, Technical report, University College Cork, Final year project report at HMRC.
- Miles, M. and Funke, E. (1989), Comparison of methods for synthesis of directional seas, *Journal of Offshore Mechanics and Arctic Engineering*, 111(1), pp. 43–48.

- Nebel, P. (1994), *Synthesis of Optimal Control of a Wave Energy Converter*, Ph.D. thesis, University of Edinburgh.
- Newland, D. (2005), *An Introduction to Random Vibrations, Spectral & Wavelet Analysis*, Dover Publications, 3rd edition.
- Newman, J. (1977), *Marine Hydrodynamics*, The MIT Press.
- Payne, G. S., Taylor, J. R., Bruce, T., and Parkin, P. (2008), Assessment of boundary-element method for modelling a free-floating sloped wave energy device. part 2: Experimental validation, *Ocean Engineering*, 35(3-4), pp. 342–357.
- Rogers, D. and Bolton King, G. (1997), *Wave generation using Ocean and wave*, Edinburgh Designs Ltd., Edinburgh, Scotland.
URL www.edesign.co.uk
- Spinneken, J. (2004), Water surface following wave gauge, Technical report, University of Edinburgh.
URL www.wavegauge.joecraft.com
- Stansfield, F. (1970), *Hydrostatic Bearings*, The Machinery Publishing Company Ltd.
- Taylor, J. and Mackay, I. (2001), The design of an eddy current dynamometer for a free-floating sloped IPS buoy, in *Marine Renewable Energy Conference (MAREC)*, pp. 67–74, The Institute of Marine Engineers, Newcastle upon Tyne, UK.
- Thompson, E. F. and Long, C. E. (1987), Wave measurement and analysis in laboratory flumes, in *IAHR Seminar on WAVE ANALYSIS AND GENERATION IN LABORATORY BASINS*, pp. 75–90, Lausanne, Switzerland.
- Thornton, E. B. and Calhoun, R. J. (1972), Spectral resolution of breakwater reflected waves, *American Society of Civil Engineers, Journal of the Waterways, Harbors and Coastal Engineering Division*, 98(WW4), pp. 443–460.
- Tuah, H. and Hudspeth, R. T. (1982), Comparisons of numerical random sea simulations, *Journal of Waterway, Port, Coastal and Ocean Engineering*, 108(WW4), pp. 569–584.
- Tucker, M. and Pitt, E. (2001), *Waves in ocean engineering*, Elsevier.
- Weber, J. (2007), Representation of non-linear aero-thermodynamic effects during small scale physical modelling of OWC WECs, in *7th European Wave and Tidal Energy Conference*, Porto, Portugal.